Reviews
Nanostructured, nanoscale materials and nanodevices

New insights into detonation synthesis and properties of nanodiamonds

© Valerii Yu. Dolmatov[a]✉, Dmitry V. Rudenko[a], Maxim N. Kiselev[b],
Nataliya P. Satonkina[c], Natalia M. Lapchuk[d], Maria A. Blinova[a,e], Vladimir T. Senyut[f],
Sergey D. Pisarevsky[g], Alla V. Nozhkina[h], Alexander P. Ershov[c]

[a] *Special Design and Technology Bureau "Tekhnolog", 33-a, Sovetsky Pr., St. Petersburg, 192076, Russian Federation,*
[b] *JSC "Plant "Selmash", 66, Shchorsa St., Kirov, 610014, Russian Federation,*
[c] *Lavrentiev Institute of Hydrodynamics of Siberian Branch of RAS,*
15, Lavrentieva Pr., Novosibirsk, 630090, Russian Federation,
[d] *Belarusian State University, 4, Nezavisimosti Av., Minsk, 220030, Belarus,*
[e] *State Institute of Technology Saint-Petersburg Russia,*
26, Moskovsky Av., St. Petersburg, 190013, Russian Federation,
[f] *The Joint Institute of Mechanical Engineering of the NAS of Belarus,*
12, Akademicheskaya St., Minsk, 220072, Belarus,
[g] *Geoinformation Systems of the NAS of Belarus, 6, Surganova St., Minsk, 220012, Belarus,*
[h] *JSC "Research Institute of Natural, Synthetic Diamonds and Tools",*
65, Gilyarovsky St., Moscow, 107996, Russian Federation

✉ diamondcentre@mail.ru

Abstract: The paper presents mainly new or previously unanalysed data from the most important published papers of the last five years. Several possible mechanisms for the synthesis of detonation nanodiamonds (DND) are considered. A simple predictive estimate of the DND yield based on the content of elements in the explosive molecule is proposed. It is shown that nitrogen is not an inert element in the nanodiamond synthesis process. It is possible to form a fractal carbon lattice with simultaneous fluctuations of carbon density in the chemical reaction zone (CRZ) with the formation of a three-dimensional ordered core in the nodes of the lattice. The time of formation of such a carbon structure is close to 50 ns. For DND formation, the time of chemical reactions is 0.1–0.3 μs, and the width of the CRZ is 0.4 to 1.4 mm. The electrical conductivity of the 'plasma' in the CRZ is determined by the carbon content of the explosives, which forms extended conducting structures. It is shown that the region with the highest DND yield (up to 8.5 wt. %) is limited by the pressure in the Chapman-Jouguet plane of 23–29 GPa and the temperature of 3850–4350 K, the optimum oxygen balance of the explosive is in the range of $-42 \div -53$ %, and the detonation velocity is in the range of 7250–8000 m·s^{-1}. In general, DNDs from different explosives have close crystallographic parameters (except for nanodiamonds from benzotrifuroxane). To increase the yield of DNDs, it is necessary to use an aqueous charge shell, which is a solution of urotropine, urea or hydrazine. For the first time, the process of DND production from Tetryl and its binary and ternary charges was developed and recommended for industry, with a DND yield of ~7 wt. %. Experience with the industrial production of DND has shown that it is realistic to obtain nanodiamonds with a yield of 8.5 wt. % at their content in the diamond containing blend of 72 % and non-combustible impurities of 1.6 wt. %.

Keywords: detonation nanodiamonds; explosives; synthesis mechanism; predictive estimation of yield; production; properties.

Новое о детонационном синтезе и свойствах наноалмазов

© В. Ю. Долматов[a]✉, Д. В. Руденко[a], М. Н. Киселев[b],
Н. П. Сатонкина[c], Н. М. Лапчук[d], М. А. Блинова[a,e], В. Т. Сенють[f],
С. Д. Писаревский[g], А. В. Ножкина[h], А. П. Ершов[c]

[a] *Специальное конструкторско-технологическое бюро «Технолог»,*
Советский пр., 33-а, Санкт-Петербург, 192076, Российская Федерация,
[b] *АО «Завод «Сельмаш», ул. Щорса, 66, Киров, 610014, Российская Федерация,*
[c] *Институт гидродинамики им. М. А. Лаврентьева СО РАН,*
пр. Лаврентьева, 15, Новосибирск, 630090, Российская Федерация,
[d] *Белорусский государственный университет, пр. Независимости, 4, Минск, 220030, Республика Беларусь,*
[e] *Санкт-Петербургский государственный технологический институт (технический университет),*
Московский пр., 26, Санкт-Петербург, 190013, Российская Федерация,
[f] *Объединенный институт машиностроения НАН Беларуси,*
ул. Академическая, 12, Минск, 220072, Республика Беларусь,
[g] *УП «Геоинформационные системы» НАН Беларуси, ул. Сурганова, 6, Минск, 220012, Республика Беларусь,*
[h] *ОАО «Научно-исследовательский институт природных, синтетических алмазов и инструмента»,*
ул. Гиляровского, 65, Москва, 107996, Российская Федерация

✉ diamondcentre@mail.ru

Аннотация: В статье изложены, в основном, новые или ранее не проанализированные данные наиболее важных опубликованных работ последних пяти лет. Рассматриваются различные возможные механизмы синтеза детонационных наноалмазов (ДНА). Предложена простая прогнозная оценка выхода ДНА на основе содержания элементов в молекуле взрывчатых веществ (ВВ). Показано, что азот не является инертным элементом в процессе синтеза наноалмазов. Возможно образование фрактальной углеродной сетки с одновременными флуктуациями плотности углерода в зоне химических реакций (ЗХР) с образованием трехмерного упорядоченного ядра в узлах сетки. Время формирования такой углеродной структуры близко к 50 нс. Для образования ДНА время химических реакций составляет 0,1…0,3 мкс, а ширина ЗХР – от 0,4 до 1,4 мм. Электропроводность «плазмы» в ЗХР определяется содержанием углерода в ВВ, который формирует протяженные проводящие структуры. Показано, что область с наибольшим выходом ДНА (до 8,5 мас. %) ограничена давлением в плоскости Чепмена-Жуге 23…29 ГПа и температурой 3850…4350 K, оптимальный кислородный баланс ВВ находится в диапазоне –42…–53 %, скорость детонации ВВ – в диапазоне 7250…8000 м/с. В целом, ДНА из различных ВВ имеют близкие кристаллографические параметры (кроме наноалмазов из бензотрифуроксана). Для повышения выхода ДНА необходимо использовать водную оболочку заряда, представляющую раствор уротропина, мочевины или гидразина. Впервые разработан и рекомендован для промышленности процесс получения ДНА из тетрила и его бинарных и тройных зарядов, выход ДНА ~7 мас. %. Опыт промышленного производства ДНА показал, что реально получение наноалмазов с выходом 8,5 мас. % при их содержании в алмазосодержащей шихте 72 % и несгораемых примесей 1,6 мас. %

Ключевые слова: детонационные наноалмазы; взрывчатые вещества; механизм синтеза; прогнозная оценка выхода; получение; свойства.

Nomenclature

BTF   – benzotrifuroxane, benzotris (1,2,5-oxadiazole-1,4,7-trioxide);

C-J   – Chapman-Jouguet plane;

CEP   – composite electrochemical coating;

CRZ   – zone of chemical reactions during explosive decomposition of explosives;

DB   – diamond detonation blend (detonation diamond-containing nanocarbon);

DND   – detonation nanodiamond;

DP   – detonation products;

EDNA – ethylene-N,N′-dinitramine, ethylene dinitramine, haleite;

EPR   – electron paramagnetic resonance;

FL   – fluorescence;

Hexyl – hexanitrodiphenylamine, dipicrylamine;

MRI   – magnetic resonance tomography;

NMR   – nuclear magnetic resonance;

NV   – nitrogen-substituted vacancy;

OB   – oxygen balance of explosives;

Octogen – cyclotetramethylenetetranitramine, 1,3,5,7-tetranitro-1,3,5,7-tetrazacyclooctane, octahydro-1,3,5,7-tetranitrotetrazine;

Pentrite – pentaerythritol tetranitrate;

PVP   – polyvinylpyrrolidone;

RDX   – hexogen (cyclotrimethylenetrinitramine),

TATB – 1,3,5-triamino-2,4,6-trinitrobenzene;

Tetryl – 2,4,6-trinitro-N-methyl-N-nitroaniline, methylpicrylnitramine, N-methyl-2,4,6-trinitrophenylnitramine;

TH   – alloys or mixtures of TNT and RDX;

TNP   – 2,4,6-trinitrophenol, picric acid;

TNT   – 2,4,6-trinitrotoluene;

Z-TAKOT – 2,4,8,10-tetranitro-5H-benzotriazolo-[2,1-a]-benzotriazoli-6-um.

1. Introduction

The detonation nanodiamond was first obtained by a group of Russian scientists consisting of K.V. Volkov, V.V. Danilenko and V.I. Yelin in 1963 [1]. Subsequently, a great contribution to the development of numerous research areas in various fields of science and technology was made by such scientists as: V.V. Danilenko, V.Yu. Dolmatov, V.M. Titov, A.Ya. Vul, A.N. Ozerin, I.I. Kulakova, A.L. Vereshchagin, E.R. Pruuel, B.V. Spitsyn, A.P. Vozniakovsky, A.M. Staver, V.G. Sushchev, V.A. Marchukov (*Russian Federation*); P.A. Vityaz, N.M. Lapchuk, V.T. Senyut (*Belarus*); N.V. Novikov, O.O. Bochechka, G.P. Bogatyreva (*Ukraine*); D.M. Gruen, Y. Gogotsi, V. Mochalin, O. Shenderova (*USA*); A.S. Barnard (*UK*); E. Osawa, T. Enoki, M. Endo, M. Sone, M. Kawasaki (*Japan*); H. Fenglei, S. Chen, S.Z. Peng, N.S. Xu (*China*); J-Ch.Arnault, V. Pechot, J.-B. Donnet (*France*); A. Shames, A. Panich (*Israel*); V. Myllymaki, A. Vehanen (*Finland*).

Since the beginning of the XXI century, a new scientific and technological direction – nanostructured materials science – has been actively created and developed, studying structures with dimensions in the range of 2–100 nm, which are significantly influencedby the properties of interfaces. The development of nanotechnologies related to the creation of nanocomposites is particularly promising. There is a major problem of stability and reproducibility of nanostructures, which always create strong and multilevel aggregates with sizes already in the micro range. As a result, as the size of

nanoparticles decreases, the dynamic instability of nanosystems increases, leading to the phenomenon of 'unrepeatability' of structures and properties in the technologies actually used.

The general reason for the emergence of new properties is that a significant proportion of the atoms of nanoparticles are located on their surface. For example, in nanodiamond particles of 2 nm size, the number of bulk and surface atoms is approximately equal (~600 atoms each). Therefore, the contribution of surface energy to the free energy of the nanoparticle is significant. Uncompensated bonding of the extraneous atoms creates an all-round compression of the particle - the so-called Laplace pressure $P = 2\sigma/R$ (where σ is the surface tension and R is the radius of the particle). This reduces the lattice parameters and leads to changes in the low temperature heat capacity, thermal conductivity, Debye temperature and superconducting transition critical temperatures. There are no dislocations in nanoparticles because the size of the dislocation loops is larger than the particle size. This means that the plasticity of the nanoparticles is greatly reduced. The change in various properties starts from a particle size in the range of 3 to 100 nm. Mechanical grinding does not produce a nanodispersed state.

There are many inconsistencies in describing the properties of DND in traditional terms suitable for characterising both diamond crystals and powders. As research on nanodiamonds continues, the dual nature of this material is becoming more apparent: as a nanocrystal of small length on the one hand, and as a self-ordered fractal cluster structure on the other.

Having undergone a complex of shock-thermal effects and chemical attacks from the gaseous medium in the blast wave, diamond-containing carbon is a substance with the most complex structural organisation. It contains crystalline formations, which continuously change into looser and less ordered spatial formations with a wide range of energy states and types of interatomic and intermolecular bonds [1–4].

The originality of the DND synthesis method lies in the fact that the carbon source for the diamond nanoparticles is the carbon atoms in the explosives molecules, i.e. negative oxygen balance explosives are used, in which there is insufficient oxygen for complete oxidation of the combustible components of the explosives (carbon and hydrogen).

Detonation nanodiamonds are an example of the diversity and inexhaustibility of the properties of the nanoworld.

The aim of the review is to systematise empirical and theoretical knowledge of the complex process of DND synthesis and to analyse data on new technologies for their production.

2. Mechanism of DND Production

A direct experiment to determine the real process of DND formation behind the detonation wave front still remains an unsolvable problem. The detonation wave is a single complex of the shock wave, in the front of which the decomposition of explosives begins, the chemical reaction zone, which follows the shock wave and ends in the Chapman-Jouguet (C-J) plane, and, finally, the Taylor unloading wave (isoentropy). Moreover, the energy release continues beyond the Chapman-Jouguet plane. The maximum pressure and temperature are reached inside the CRZ. It has been shown in many studies [5–9] that the process of nanodiamond formation proceeds in the CRZ and is completed at the beginning of the Taylor expansion of detonation products (DPs), i.e., during the process of the dispersion of DPs, DND crystallites first continue to grow and only after a sharp drop in pressure and temperature and a decrease in the concentration of active carbon radicals does their growth stop.

2.1. The chemical reaction zone during detonation synthesis of nanodiamonds on the carbon phase diagram [10]

Looking at the classical P, T carbon diagram, the free carbon from TNT ($P \sim 18$ GPa, $T \sim 3600$ K, DND yield ~1 wt. %) is clearly not in the liquid carbon state, but the free carbon from BTF (benzotrifuroxane) ($P \sim 36$ GPa, $T \sim 4500$ K, DND yield ~1 wt. %) [10] – on the contrary – falls into the liquid carbon state.

On the classical carbon phase diagram (CPD), the limits of possible DND production are defined by pressures between 15 and 38 GPa and temperatures between 3000 and 4400 K. However, for theoretical and practical purposes, a more precise pressure and temperature range is required.

Thus, new data on DND yield, pressure and temperature in the C-J plane, composition of explosive charges, taking into account their oxygen balance and optimum density, plotted on CPD, showed that the range with the highest DND yield is limited by pressure in the C-J plane of 23–29 GPa and temperature of 3850–4350 K, DND yield in this range is usually between 6.1 and 8.2 wt. % (Fig. 1).

When nanodiamonds are obtained, an aqueous charge shell is used and the oxygen balance of the explosives should be in the range of –42÷–53 %.

Since the use of explosives is a hazardous process and not all suitable explosives are readily available for the production of DND, it is reasonable to consider the theoretical possibility of using explosives. There are currently only two known methods of producing DND – from a mixture of TNT and RDX and from Tetryl [11], but due to the increasing cost of raw materials (explosives) and their scarcity, it has become necessary to search for new, more affordable types of explosives [12]. The best known characteristics of explosives are detonation velocity and OB. In [13] it was found that for some aromatic nitro compounds (explosives), the optimum OB for producing DND with a yield ≥ 5 % of the explosive mass is –35÷–60 %. These data can be used with a high degree of confidence by relating this value to the detonation velocity of the explosives, since [14] showed the dependence of the DND yield on the detonation velocity of a number of aromatic nitro compounds (mainly mixtures of TNT and RDX) with an optimum of 7250–8000 m·s^{-1} (DND yield ≥ 5 wt. % of the explosive). Figure 2 [15] shows the region bounded by OB = 35÷–60 % and the optimum detonation velocity of 7250–8000 m·s^{-1} in the detonation velocity-oxygen balance coordinates.

All explosives in this region (as well as those immediately beyond) are likely to give an acceptable DND yield (≥ 5 wt. %). These new starting explosives include: hexyl (hexanitrodiphenylamine), hexanitrodiphenyl, tetranitroaniline, tetranitrobenzene, trinitroaniline, trinitroanisole, 1,3-diamino-2,4,6-trinitrobenzene, trinitrobenzene and mixtures thereof.

The explosion parameters and yield achieved for some explosives are given in Table 1.
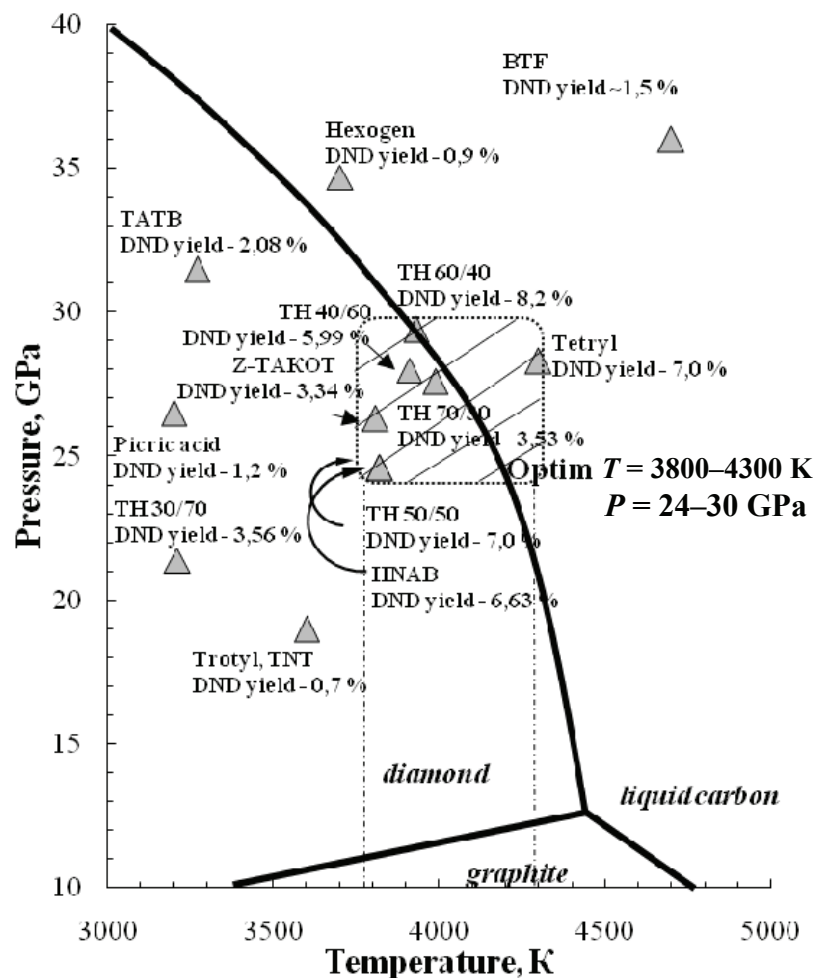
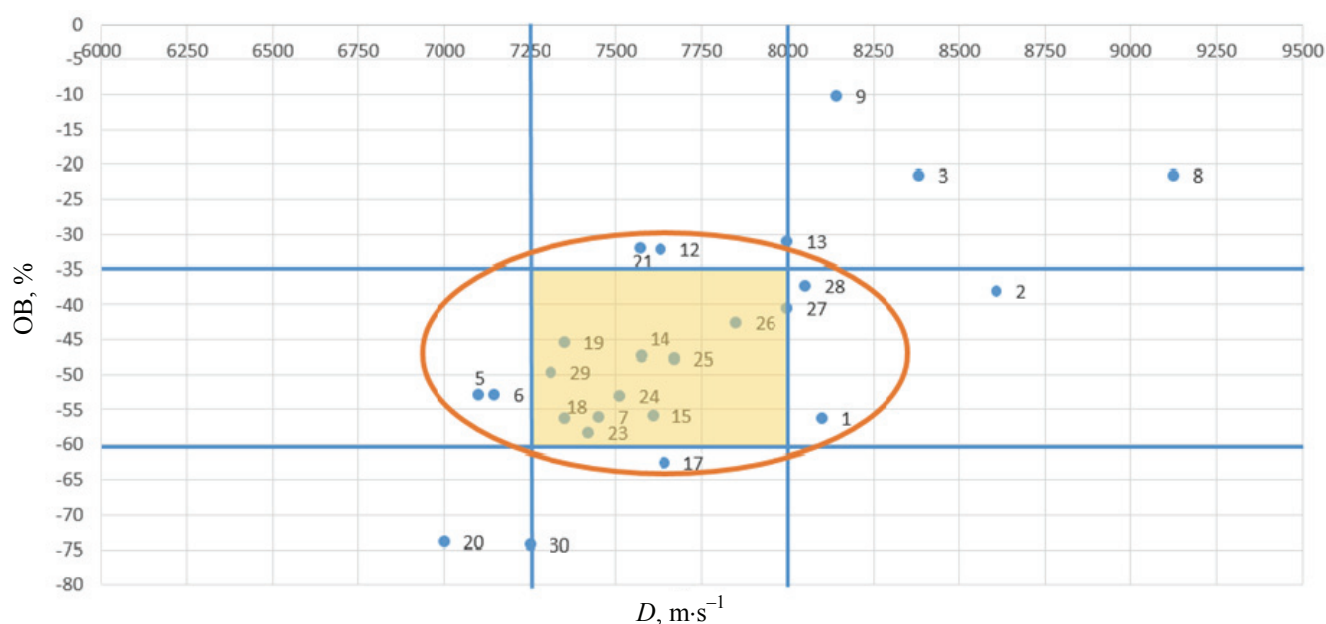**Fig. 1.** Dependence of DND yield on *P, T* – conditions on the carbon phase diagram

Fig. 2. Detonation rate and oxygen balance of explosives optimal for producing DND with yields ≥ 5 wt. % of explosives

Table 1. Detonation rate, oxygen balance,
and DND yield depending on the type of explosives [1, 3, 6, 9, 15]

No.	Explosive	D, m·s^{-1}	OB, %	DND yield, %
1	Aminotrinitrobenzene (trinitroaniline)	8100	−56.16	
2	BTF	8610	−38.08	~1.0
3	RDX	8383 8850	−21.6	~1.0
4	Hexanitrodiphenyl	7100	−52.8	
5	Hexyl	7145	−52.8	
6	1,3-diamino-2,4,6-trinitrobenzene	7450	−55.97	
7	Octogen	9124	−21.6	~1.0
8	Pentrite	8142 8277 8590	−10.1	0.15
9	Tetranitroaniline	7630	−32.2	
10	Trinitrobenzene	8000	−31	
11	Tetryl	7573	−47.4	7.6
12	TATB	7606 7970	−55.8	4.1
13	Trinitroanisole	7640	−62.5	
14	Trinitrobenzene	7350	−56.3	
15	Trinitrophenol (picricacid)	7350	−45.4	~1.5
16	TNT	7000	−73.9	~1.0
17	EDNA	7570 7750	−32	
18	TH 70/30	7420	−58.3	4.7
19	TH 60/40	7510	−53	8.5
20	TH 50/50	7670	−47.8	6.0
21	TH 40/60	7850	−42.6	5.8
22	TH 36/64 (press.)	8000	−40.5	5.4
23	TH 30/70	8052	−37.3	4.4
24	bis-(2,4,6-trinitrophenyl)-diazine	7311	−49.6	6.63
25	Z-TAKOT	7250	−74.2	3.34

2.2. Some theoretical and experimental ideas about the mechanism of DND synthesis

There are different views on the process of DND formation. According to [16, 17], the method of small-angle X-ray scattering (SAXS) allowed to study the increase in size of the formed carbon particles from the moment of passing the detonation front. Immediately after the detonation wavefront, a carbon nanoparticle with a size of ~1.0–1.5 nm is recorded. The particle size continues to increase, reaching sizes of ~2.5–3.0 (TATB), ~6.0–7.2 (TH 50/50) and ~7.0 nm (BTF) within ~3–4 μs (Table 2).

It should be noted that the small-angle X-ray scattering method only allows the size of particles to be determined, and other methods should be used to determine their graphite or diamond structure.

Table 2. DND particle size depending on the type of explosive

Explosive	TATB	TH 50/50	BTF
d, nm	~2.8	~6 − 7	~7.2

The idea that in CRZ there is a complete destruction of explosive molecules into atoms is unrealistic [18–20]. The fact is that breaking only C–C, C–H and C–N bonds in TNT requires ~23,900 kJ·kg^{-1}, and the heat of explosive decomposition is only 4312 kJ·kg^{-1}, i.e. 5.5 times less [20].

Breaking C–H and C–N bonds in RDX requires ~19400 kJ·kg^{-1}, and the heat of explosive decomposition is about 5740 kJ·kg^{-1}, i.e. 3.8 times less. Breaking C–C and C=N bonds in hydrogen-free benzotrifuroxane requires 24600 kJ·kg^{-1} and its heat of decomposition is only 5860 kJ·kg^{-1}, i.e. 4.2 times less. Thus, the ideas associated with homogenisation of "free" carbon atoms and their subsequent condensation into an amorphous carbon phase in combination with liquid-drop coalescence or with coagulation and crystallisation of carbon at expansion isoentropy are not realistic as the sole or main mechanism of DND formation. The decomposition of explosives is a very complex multi-stage set of successive and parallel redox reactions.

During detonation, the chemical equilibrium in the DP does not have time to establish itself because the reactions do not proceed to completion and the DP contains a significant amount of intermediates. The composition of the DP is also affected by changes in the initial charge density. Experimental determination of the composition of cold DP does not provide information about the composition of DP in the Chapman-Jouguet plane, since the DP composition is subject to change during expansion and cooling.

According to the authors [18], there may be more than one mechanism for the formation of DND crystallites. The formation of primary fragments of future nanodiamonds starts from the beginning to the end of the CRZ (up to the Chapman-Jouguet plane). It is assumed that a sufficiently stable formation in the CRZ plasma is a multi-carbon radical dimer with a –C–C– covalent bond.

Crystallization of nanosized diamond in CRZ is impossible due to practically no heat dissipation from the formed nanoparticle and short time of existence of necessary P, T conditions. There is a process of self-organization of carbon into condensed phase in accordance with the basic chemical properties of carbon atoms, namely the formation of various types of C–C bonds.

The paper [21] suggests the formation of a fractal carbon lattice with fluctuations of carbon density in the plasma of the chemical reaction zone during the explosive decomposition of explosives. In the "nodes" of this grid, the carbon condensate with the highest density manages to form a three-dimensional ordered core, while the areas with lower carbon density are repeatedly destroyed and recombined in the process of DP dispersion. Thus, it is likely that the prastructure of DND can be either a compacted plasma-like carbon core that becomes liquid carbon beyond the C-J plane, or a formed energetically favorable carbon framework of cyclohexane that is rearranged beyond the C-J plane into a radical molecule of adamantane attacked by C_2 radicals by interacting with each other with even greater energy reduction (diffusion mechanism of nanodiamond formation). It is possible that these two mechanisms of DND formation take place. Furthermore, there is crystallization or amorphization of liquid carbon, and cooling of DND crystallites obtained by diffusion from the adamantane structure may occur.

The growth of DND particles occurs by a diffuse mechanism due to chemical reactions that occur on their surface during C_2 attack. The spatial arrangement of carbon atoms in the adamantane molecule repeats the arrangement of atoms in the diamond crystal lattice. The uniqueness of the adamantane molecule is that it is highly symmetrical and thermally stable. According to [18], the detonation of hydrogen-containing explosives results in the competitive formation of nanodiamond crystallites from radical-like C_2 dimers and methyl radicals from the methyl group of TNT.

Only in the future, after the creation of new instrumental methods for the analysis of fast processes, it will be possible to determine the real mechanism of DND crystallite formation.

The detonation transformation of an explosive, now and in the future, cannot be described by a simple and specific dependence. The oxidizer (oxygen of the explosive molecules) in the detonation wavefront and up to the Chapman-Jouguet plane (the width of the chemical reaction zone is ~0.6 mm, and the process time is 0.1–0.3 μs) interacts with the propellant (carbon and hydrogen in the explosive molecules), creating the necessary P, T conditions for the coagulation of nanodroplets of "extra" carbon (or the growth of DND particles by the diffusion mechanism) in the chemical reaction zone. Beyond the Chapman-Jouguet plane, these nanodroplets coalesce into larger ones and, depending on the P, T conditions, crystallize as nanodiamonds or amorphize

upon cooling. In [21], only the simplest and most obvious data – the mass content of all elements, carbon, hydrogen, nitrogen and oxygen in the molecules of carbon-containing single and mixed explosives of the general formula $C_aH_bN_cO_d$ – can be used for predictive evaluation.

The dome-shaped dependence of the DND yield on the carbon content of the explosives (Fig. 3) determines the amount of carbon (23–34 wt. %) in combination with oxygen that is necessary and sufficient to achieve an acceptable nanodiamond yield (greater than 5 wt. % of the explosives mass). Hydrogen (1.5–3.0 %), as well as some of the burnt carbon, is combustible for the oxygen of the explosives to release additional energy to provide the necessary *P, T* conditions in the chemical reaction zone (CRZ). The amount of oxidizer (oxygen) has its optimum (42–46 wt. %) to provide the required amount of energy in the CRZ, sufficient to provide the necessary *P, T* conditions for the formation of the DND structure in the CRZ.

Nitrogen is considered to be an inert element for explosive processes, but the clearly pronounced dome-shaped dependence of the DND yield on its content in explosives (23–31 wt. %) (Fig. 3) shows that this is not the case. This is further confirmed by the anomalously high amount of nitrogen in DND crystallites (~2.5 wt. %).

To obtain an acceptable yield in industrial conditions more than 5 wt. %, the following conditions must be simultaneously met: hydrogen content in the explosives is ~1.5–3.0 wt. %, carbon ~23–34 wt. %, nitrogen ~ 23–31 wt. % and oxygen ~42–46 wt. % (Fig. 3). The dependence is purely empirical, but very simple and convenient in operation.

The optimum DND content in DB – from 45 to 71 wt. % is achieved in the presence of carbon from 26 to 31 wt. % in the explosive's molecules.

The carbon plasma beyond the Chapman-Jouguet plane first becomes liquid carbon and then crystallizes into DND crystallites. The crystallization process is completed in the range of 1/3–3/4 of the charge diameter from the detonation wavefront (for a 12 mm diameter charge).
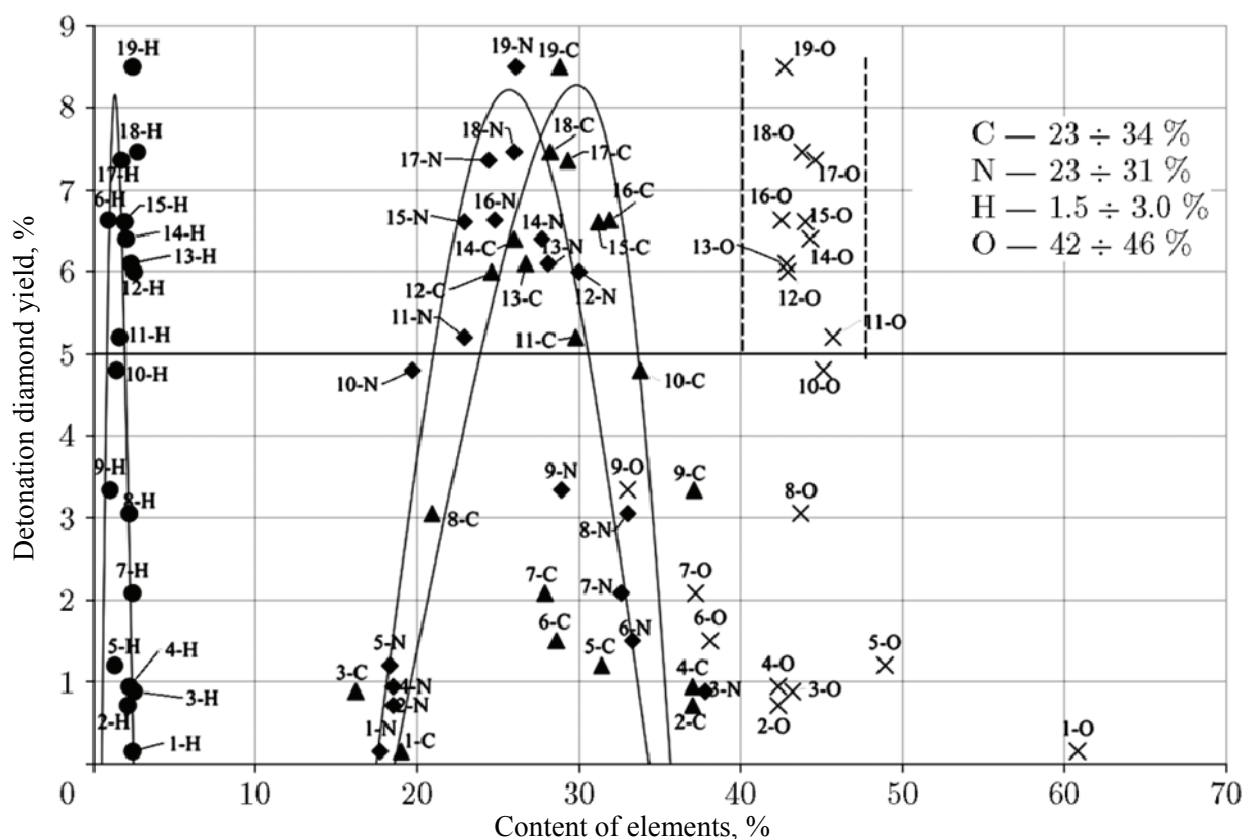

Fig. 3. Dependence of the DND yield on the content of carbon, hydrogen, nitrogen and oxygen in the molecules of the explosive

In [21] it was concluded that:

1. It was assumed that condensed carbon in the chemical reaction zone should have a density in the range of 2.5–3.2 g·cm^{-3}, in accordance with its determination in plasma by the SAXS method.

2. Probable occurrence of a fractal carbon lattice with simultaneous fluctuations of carbon density in the CRZ with formation of a three-dimensional ordered core in the nodes of the lattice.

3. For DND formation, the time of chemical reactions in the CRZ is within 0.1–0.3 μs, and the width of the CRZ is from 0.4 to 1.4 mm.

4. The formation of nanodiamonds occurs at a distance from the detonation wavefront of 1/3–3/4 of the charge diameter (for a ⌀12 mm charge).

5. The highest DND yield (more than 6 wt. %) is achieved when its formation consumes (20 ± 2) wt. % of the total carbon of the explosive.

2.3. Reaction zone electrical conductivity diagnostics

The specifics of nanodiamond formation in a detonation wave, as well as details of the kinetics of chemical reactions, remain poorly understood [22]. In condensed explosives, the CRZ is mainly studied using numerical methods. The complexity of the experimental study of the reaction zone during the detonation of condensed explosives is related to the highly aggressive medium formed in the detonation process, which also occurs in extremely narrow time frames - in fractions of a microsecond. An additional stimulus for the study of CRZ is the fact that as a result of the detonation of organic explosives, such a physical object as DND is formed in the reaction zone.

Micrographs of DND obtained with the classical 50 : 50 mixture of TH and anhydrous BTF are shown in Fig. 4. Whereas in the case of the first hydrogenated explosives, the crystallites had an average size of 5 nm, the spherical sintered crystalline DND particle size was ~100 nm when BTF was used. The spherical particle is formed by the combined effect of very high temperature (4300 K) and pressure (36 GPa) behind the detonation wavefront and the Chapman-Jouguet plane.

Experimental methods developed so far to study the reaction zone provide mostly qualitative information about the width of the reaction zone and profiles of parameters in this zone. Often the results of different methods contradict each other [23, 24].

The situation of uncertainty in the reaction zone duration is not surprising, since the reaction zone problem is one of the most complicated in explosion physics. The high reaction rate requires the measurement method to have an adequate spatial resolution. However, the extreme detonation parameters and the aggressiveness of the explosion do not allow the use of small sensors. In optical methods, which are free from these limitations, the wave interacts with the window material, which can affect the process.
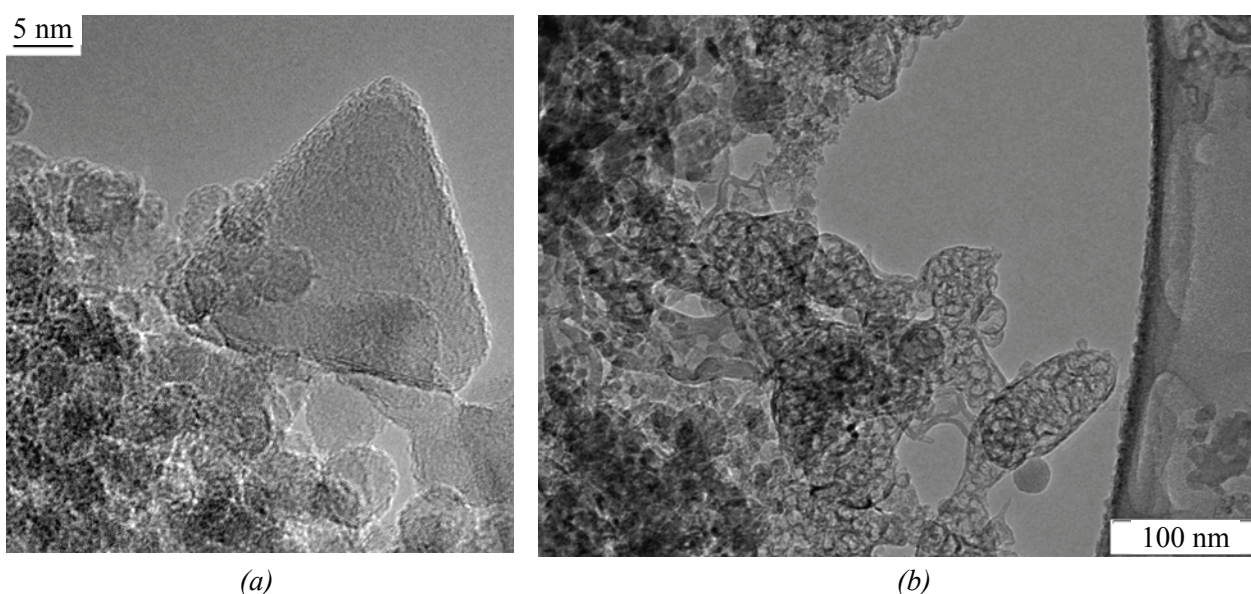

(a)   *(b)*

Fig. 4. *a* – a placer of nanodispersed diamonds obtained by detonation of boron-doped Tetryl, showing a nanodiamond with a unique shape close to an equilateral triangle with a side of about 25 nm; *b* – preserved detonation products of BTF [22]

Substance with a density of about 3 g·cm^{-3} (with the maximum crystalline density 30 % lower), is at a pressure of the order of tens of GPa and a temperature of 3000–4000 K, which is comparable to the parameters inside space objects – planets. The state of matter in the CRZ does not correspond to the classical plasma, gas, liquid or solid and cannot be described theoretically. The lack of a reliable theoretical description, together with the above factors, makes the task of a detailed experimental study of the reaction zone extremely demanding. Such matter most closely resembles the so-called warm dense matter, a state of matter at the boundary between condensed state physics and plasma: the density varies from solid (crystalline) to ten times its value, and the temperature ranges from 0.1 to 100 eV [25, 26].

Thus, when describing the reaction zone in the detonation wave, there are no small parameters that can be neglected. As shown in previous works [25–28], the electrical conductivity during the detonation of a $C_aH_bN_cO_d$ type explosive is determined by the carbon content, which, condensing just behind the detonation front, forms extended conductive structures. By measuring the conductivity of these structures, it is possible to diagnose the state of the conductive form of carbon and thus study the reaction zone. A typical conductivity profile during the detonation of a high-order explosive is shown in Fig. 5. The conductivity distribution begins with a rapid rise to a maximum value. As shown previously [27–30], the maximum electrical conductivity σ for explosive mixtures depends on several factors, including the dispersibility of the components. The growth reflects the formation of conductive carbon structures that reach the lowest resistance within the reaction zone. The region of high conductivity correlates with the reaction zone. The decrease in the value of σ(t) is related to the processes in the reaction zone and reflects oxidative processes with carbon, when carbon oxidation starts from the boundary of the structure, which leads to thinning and destruction of carbon "wires" and a decrease in the value of electrical conductivity. The duration of the reaction zone, according to the conductivity data, for high-order explosives is about 50 ns. Thus, the time of formation of a dense carbon structure is close to 50 ns.

Figure 6 shows the dependence of the maximum value of electrical conductivity on the mass fraction of carbon in the molecule of an explosive, the growth of electrical conductivity with increasing carbon content is clearly traced.
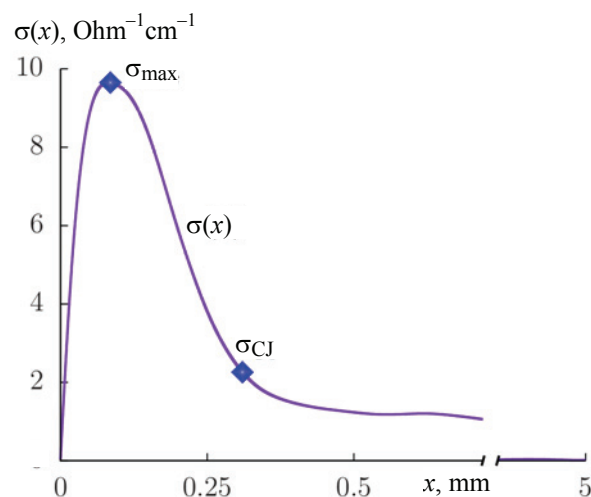

Fig. 5. Dependence of the electrical conductivity σ(x) on the coordinate x behind the detonation front obtained during detonation of a pentrite charge with a density of 1.72 g·cm^{-3}; the designation σ_{max} corresponds to the maximum value of the electrical conductivity, σ_{CJ} – to the value of the electrical conductivity spatially corresponding to the place of the end of the chemical reaction zone (Chapman-Jouguet plane) [24]

$C_aH_bN_cO_d$ type explosives have different thermodynamic parameters and carbon content in the molecule. On the one hand, more carbon means that there is more potential "fuel" for nanodiamond. On the other hand, as the carbon content increases, the values of thermodynamic parameters may decrease, so that the substance may not reach the state at which DND formation occurs.
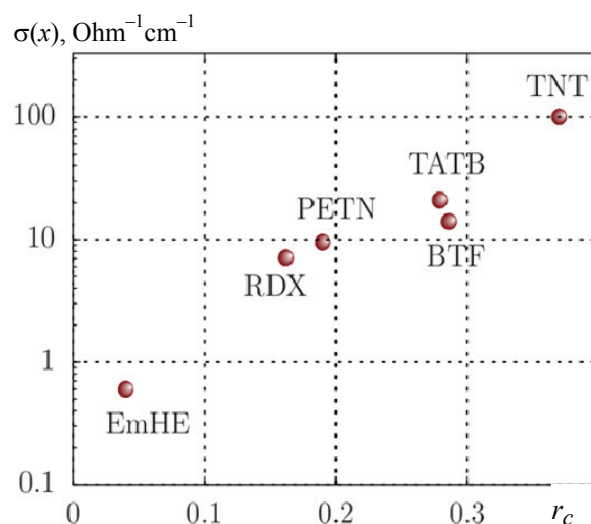

Fig. 6. Dependence of the maximum value of electrical conductivity σ_{max} obtained experimentally at close to maximum charge density on the mass fraction of carbon r_c in the explosives molecule (EmHe – emulsion explosives) [30]

On average, nanodiamonds from the preserved products of different explosives look similar. However, there is one substance formed at detonation which is more rich in size and configurations (Fig. 4*b*) – this is BTF ($C_6N_6O_6$), which has no hydrogen in its composition.

2.4. Regularities of the detonation synthesis of nanodiamonds

To date, a number of regularities reflecting the influence of synthesis parameters on the post-explosion yield of DND and diamond blend have been established [1, 31–36]. The most important parameters include
– the content of explosive components and their specific power;
  – influence of additives in the explosive charge;
  – value of the OB of the charge;
  – charge density;
  – composition and heat capacity of the gas atmosphere in the blast chamber and its composition;
  – the ratio of the chamber volume to the mass of the explosive charge.

When choosing the composition of the explosive charge, it is necessary, first of all, to proceed from economic factors – to use mass-produced explosives with a low price. The nomenclature of such individual explosives is small and, first of all, it is TNT and RDX. If using these individual explosives the DND yield is very low (0.7–0.9 and 0.3–1.0 wt. %, respectively), then from the mixture of these explosives (~60/40) the DND yield reaches 8.5 wt. % at other optimal parameters. Of the individual explosives, only Tetryl gives a DND yield higher than 7.0 wt. %, but the production of Tetryl is currently lacking, and the same yield is given by binary [34] and ternary mixtures based on Tetryl.

The optimum DND yield in terms of production cost and reduction of the load on the chemical purification stage can be considered to be 5.0–8.5 wt. % when using explosives with an oxygen balance of –35 to –55 % and charges with a density of 1.60–1.70 g·cm^{-3} [31]. Thus, it can be concluded that in order to obtain DND with a stable yield of 5 wt. % or more, it is necessary that the explosives (or a mixture of them) meet the following conditions: oxygen balance in the range of –35 to –55 %; charge density > 1.6 g·cm^{-3}.

The experience of industrial production of DB and DND under the established optimal process parameters using TH 50 : 50 and a shell from a solution of urotropine in water showed that it is possible to achieve DB yield up to 12 wt. % and DND content in the blend up to 72 wt. % (nanodiamond yield using TH 60 : 40 – up to 8.5 wt. %). After chemical purification of DND with nitric acid at the temperature of 220 °C and pressures up to 100 atm. the content of non-combustible impurities decreases 5–8 times, so it is very important to study the possibility of reducing their amount at the synthesis stage by modifying the aqueous shell of TH charges with various compounds [13].

The yield of DND (6.9 wt. %) and DB (13.4 wt. %) was achieved with the use of charge armor (shell) with a solution of urotropine in water. The use of a charge shell in the form of an aqueous solution of hydrazine and urea leads to almost identical yield of nanodiamonds (6.2 and 6.9 wt. %, respectively). The use of solutions of the above compounds in water as a shell of explosive charges leads to an average threefold decrease in the content of impurities in nanodiamonds compared to the use of a shell of distilled water.

The non-oxidizing gas medium in the blast chamber should have the highest possible heat capacity; it is best to use CO_2, but in practice, basin-shaped detonation products from previous detonations of explosive charges are used.

2.5. Synthesis of detonation nanodiamonds from single explosives and Tetryl-based compositions

The process of DND production from commercially available picric acid (TNP) was investigated for the first time in two variants: TNP stabilized with 7.5 % H_2O and dry TNP (more dangerous in handling). Despite the presence of an aqueous shell, the yield of DND is also low in this case, 0.46 and 1.2 wt. %, respectively. Thus, the use of picric acid for the industrial production of DND is not economically efficient [34, 37].

In order to compare new possibilities of DND synthesis from Tetryl (in aqueous or aqueous-urotropine shell), DND synthesis was first carried out in a gaseous medium (nitrogen). The yield of DND was very low (0.37 wt. %) and unsuitable for industrial production. The use of a new variant – aqueous or aqueous-urotropine shell under the same synthesis conditions allowed to increase the yield ~ 20 times up to 6.3–7.1 wt. % with the amount of noncombustible impurities 0.38–0.95 wt. % [34, 37, 38].

This method, taking into account the large reserves of conversion Tetryl, can be recommended for industrial production of DND. The aqueous shell of the charge allows for efficient heat removal in postdetonation processes while preserving the DND.

The use of urotropine allows to maintain a reducing environment in the blast chamber, and also protects DND from the oxidizing effect of aggressive gases – CO_2 and H_2O – under blast conditions. Urotropine acts as a target for aggressive gases, thus protecting DND.

The new method of DND production from Tetryl allows to obtain nanodiamond with high yield (6–7 wt. %) and high DND content in the diamond blend (51–63 wt. %), which significantly simplifies the chemical purification of DND. DND-enriched diamond blend can be used as a modifying additive in polymer chemistry, electroplating, oils and lubricants without additional treatment.

2.5.1. Binary compositions

Binary compositions with Tetryl, at its content of more than 50 wt. % with TNT, RDX and picric acid give DND yields in the range of 5.2–7.34 % (average – 6.1 %) [35]. The yield of DB ranges from 10.0 to 16.2 wt. %. Thus, in terms of absolute DND yield, the leader is single Tetryl – 7.05 %, followed by binary charges – 6.1 %.

TNT is the most effective additive to Tetryl, RDX is slightly inferior to it, and the lowest DND yield is obtained when picric acid is used as an additive.

Figure 7 shows the X-ray diffractogram of DND from TH 50/50 in aqueous solution, non-combustible impurities < 0.1 % (I), and from pure Tetryl, non-combustible impurities 0.46 % (II).
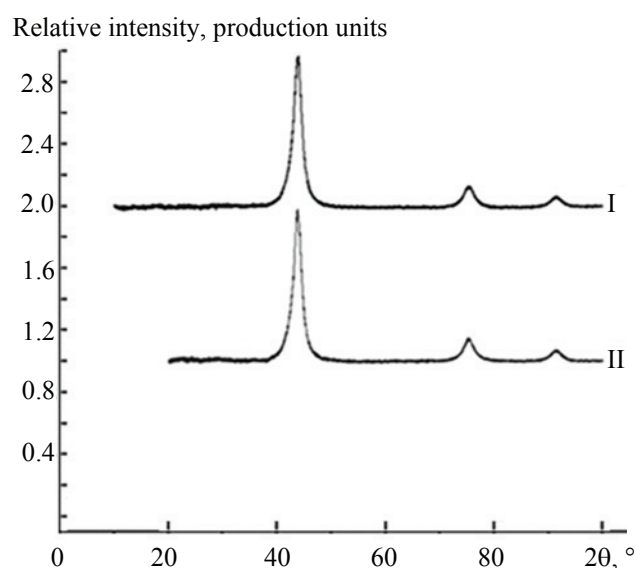
Relative intensity, production units

Fig. 7. DND diffractograms: I – from a 50/50 TH in aqueous solution of urotropine; II – from pure Tetryl in aqueous solution of urotropine

The degree of perfection of the crystal structure of DND depends on the conditions of detonation synthesis. Thus, the diffractogram of diamond obtained from Tetryl is characterized by a set of three reflections (111), (220) and (311) of cubic polytype and is identical to the classical DND obtained from a 50/50 TH charge.

2.5.2. Synthesis of DNDs from Tetryl-based ternary charges

Ternary compositions of explosives allow for more precise adjustment of oxygen balance and power by different combinations of three explosives, increased density by different particle size distributions of the starting explosives, and ultimately a higher yield of DND [36]. In addition, even partial replacement of expensive and scarce RDX with conversion Tetryl is economically feasible.

It is shown that the use of the ternary mixture practically does not worsen the sensitivity indices of explosive mixtures in comparison with the TH-50 mixture. Taking into account the somewhat lower chemical resistance of the compositions, it is expedient to make charges from the ternary mixture by pressing. Comparative experiments on a pilot scale (composition of TH 50/50 and TH 60/40 (aqueous and aqueous-urotropine armor) showed that the DND yield of 6.74–7.50 wt. % is lower than from complex three-component charges – Tetryl, TNT and RDX (DND yield ~8.0 wt. %). When the binary charge contains 50 wt. % or more of Tetryl, the range of DND yield data is large – from 4.8 to 7.3 wt. %. When using ternary charges, the DND yield is much higher and its variations are not significant – 7.6–8.2 wt. %, which shows a near-optimal combination of oxygen balance and specific power of the explosive charge, providing the highest yield of nanodiamonds.

Thus, it is possible to recommend to use pressed charges from a mixture of Tetryl and (TNT + RDX) with the content of the former from 50 to 75 wt. %; further it is necessary to economically justify the most optimal charge from a ternary mixture – Tetryl, TNT and RDX, taking into account, first of all, the scarcity and high price of RDX.

3. Properties and purification of diamond detonation blend

DB is a detonation synthesis product containing diamond-like carbon structures and various graphite-like structures. The main part of non-diamond forms of carbon is located on the surface of the diamond

core, the fragments of which are connected not only physically but also by chemical bonds. It is impossible to separate nanodiamonds without chemical treatment, which provides an energetic impact sufficient to break the strong carbon-carbon bonds.

Chemical purification is the most expensive and complex step in the production of nanodiamonds. The purification technology determines the performance characteristics of nanodiamonds and the cost level of DND and its availability for various applications. During the transition from DB to nanodiamonds, the textural properties of the substance do not change monotonically, but discontinuously, which distinguishes the mixture from other carbon materials [39].

Chemical purification of DB in the liquid phase combines the processes of oxidation and acid dissolution of impurity metals and is the most effective. In [40] the treatment of DB with an aqueous solution of ammonium nitrate in weak nitric acid is proposed. NH_4NO_3 is used in significant excess in relation to the mixture – 10–15 wt. % of ammonium nitrate per 1 wt. % of DB. The process is carried out at a temperature of ~220 °C until the end of gas emission, which indicates the completion of the oxidation process and decomposition of NH_4NO_3. The decomposition of ammonium nitrate under oxidation conditions leads to nitrogen, and the released oxygen is used for oxidation of non-diamond carbon. The presence of nitric acid in the reaction mixture provides dissolution of metal impurities in the form of soluble metal nitrates (impurities).

The advantage of the process is the absence of toxic nitrogen dioxide in the gaseous reaction products, which makes it possible to completely abandon expensive systems for absorption and regeneration of nitric acid. In addition, the low content of nitric acid in the spent reaction mass makes it possible to dispense completely with acid regeneration.

In [41], two variants of detonation nanodiamond blend powders doped with 0.96 and 0.73 wt. % boron were prepared by detonation using a 50/50 mixture of TNT and RDX or Tetryl, respectively. Their morphology, texture and mesostructure were investigated by scanning electron microscopy, small-angle neutron scattering and low temperature nitrogen adsorption techniques. It was found that there is a significant influence of the explosion precursor on the structure and morphology of the obtained carbon nanopowders.

A comprehensive analysis of the obtained data revealed the presence of mesoporous powders consisting of randomly oriented non-spherical (anisodiametric) nanoparticles of lamellar shape of approximately equal thickness ($T \approx 25$ Å – when using TNT and RDX and 28 Å – for Tetryl), differing by a significantly smaller width when using Tetryl ($W > 550$ and ≈ 136 Å, respectively).

It was found that DB obtained from a mixture of TNT and RDX is characterized by a 2-fold higher specific pore volume (1.14 *vs*. 0.8 $cm^3 \cdot g^{-1}$) and a 1.5-fold higher specific surface area (296 *vs*. 184 $m^2 \cdot g^{-1}$). It is revealed that the DB powder obtained from Tetryl is characterized by: lower homogeneity, diffuse surface of nanoparticles and bimodal pore size distribution ($d_{av} \sim 3$ and 11 nm), in contrast to the blend obtained from a mixture of TNT and RDX, which is characterized by normal pore size distribution ($d_{av} \sim 9$ nm) and smoother surface of nanoparticles. Thus, it is shown that the composition of detonation charges has a significant influence on the morphology, texture, and mesostructure of boron-doped detonation nanodiamond blend powders.

4. Properties of detonation nanodiamonds

In the detonation process, as a rule, there is enough time to form diamond nanoparticles with an average size of 4–6 nm. The carbon part is represented by a diamond core surrounded by a non-diamond carbon shell with which a layer of surface functional groups is associated (Fig. 8). DND is a gray powder containing aggregates of primary particles of different sizes and strength [1–4]. The content of impurities depends on the conditions of DND synthesis, methods of its purification and subsequent modification [42–49]. On average, DND contains oxygen (up to 7 %), hydrogen (0.4–1.8 %), nitrogen (~2.5 %), and technogenic contaminants – noncombustible residue (0.3–7.0 %) consisting of oxides and salts of Fe, Cr, Cu, Ca, Si, and others, and, as a result of corrosion of chamber walls, remnants of conductive wires and detonator primer. Oxygen, nitrogen, and hydrogen are partially included in the compounds sorbed on DND (carbon oxides, nitrogen, water, etc.), which can be located on the accessible surface or be "bricked up" in the closed pores of nanoparticle aggregates. Another part of these atoms is part of the surface functional groups. Functional groups can be eliminated or exchanged for others, but they are always present on the surface of DND.
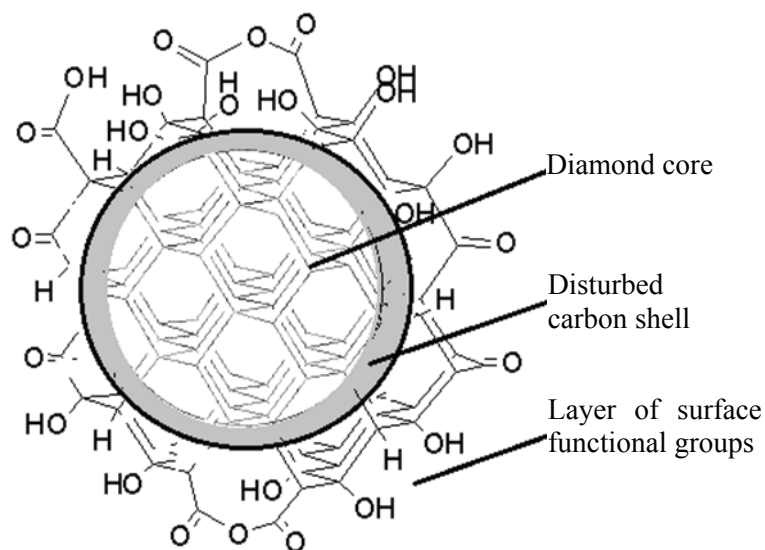
Fig. 8. A plausible model of the structure of a primary DND particle [50]

Nitrogen is present in the crystallite and as a vacancy NV center, but most of nitrogen and hydrogen are dissolved in diamond during its formation. This is proved by the fact that the results of the analysis of the basin-shaped phase composition during mechanical fragmentation of DND in vacuum showed a significant amount of nitrogen and hydrogen molecules.

The symbate dependency of the yield of carbon dioxide and nitrogen during oxidation of DND to complete oxidation of the sample indicates that nitrogen is uniformly distributed throughout the DND particle volume.

The powder contains significant amounts of oxygen, hydrogen and nitrogen atoms that are predominantly chemically bound or physically retained on the particle surface.

Nanodiamond contains 90–97 % of carbon atoms (mainly in diamond modification), surface oxygen atoms as part of functional groups (3.0–4.5 wt. %); hydrogen atoms (0.6–2.2 wt. %) both as part of functional groups and in dissolved state; nitrogen atoms in the amount of 1.8–2.8 wt. % (mainly dissolved in crystallite) and non-combustible impurities (0.04–6.0 wt. %). The composition of incombustible impurities mainly includes oxides of iron, calcium, titanium, copper, chromium, silicon and others. Hard to remove impurities are mainly titanium, silicon, lead [43, 45, 49–53].

The structure of the DND crystallite shell depends on many conditions of synthesis and chemical purification and can vary greatly in nanodiamonds from different manufacturers [13, 43, 44, 50, 52].

It was found that in a primary diamond particle of approximately 5 nm in size, the inner diameter of the diamond phase is approximately 3 nm, and the thickness of the disturbed carbon shell of the core is approximately 1 nm. The transition from the diamond core to the carbon shell is gradual, since no abrupt change in the crystal potential has been observed.

In [52] it was shown that during the oxidation of DND particles (almost to the complete oxidation of the substancr) there is symbate emission of carbon dioxide and nitrogen. This clearly indicates that nitrogen, which is not a part of the functional groups, is uniformly distributed throughout the entire volume of the DND particle.

The factor limiting the growth (≤ 8 nm) of the diamond core in DND is the violation of long-range order in DND, the accumulation of defects in the crystal structure as the carbon nanoparticle grows [54]. Comparison of the distribution of carbon atoms in DND and in defect-free diamond shows that in nanoscale diamond there is a change in the coordination number (CN) in the external coordination spheres (CS). There are "voids" – the absence of carbon atoms (lattice defects) in the CSs, which changes the structure and morphology of the DND surface. And defective structures are more reactive and more easily oxidized during chemical treatment.

In addition to the above functional groups, depending on the processing conditions, halogen- and nitrogen-containing groups (amine, amide, cyano, and nitro groups), sulfone, and other groups may be bound to the surface of nanodiamonds [53, 55–59].

4.1. Magnetic resonance study of novel detonation nanodiamonds obtained from unconventional explosives

DND are usually synthesized from a mixture of TNT and RDX. It is generally accepted that the internal structure of DND, consisting of a diamond core covered by a partially disordered shell, is very similar in all DND. The variation of DND properties is usually due to surface modification with different chemicals to obtain nanodiamonds with different properties. In [60], EPR and NMR of new DNDs synthesized from unconventional explosives not previously used for this purpose were investigated. DNDs synthesized from different explosives are shown to have different ratios of carbon atoms in the core and shell. Changes in this ratio correlate well with changes in paramagnetic defect content and ^{13}C nuclear spin lattice relaxation rates. The data presented open new possibilities for the synthesis of DNDs with desired properties.

The modification of DND properties is usually associated with surface functionalization with different chemicals to obtain various nanodiamonds such as hydrogenated, hydroxylated, carboxylated, fluorinated, chlorinated, and grafted with transition and rare earth ions [61–67].

The synthesis of DND from TNT and RDX and subsequent purification from non-diamond carbon is a relatively simple and well-established process [1, 68]. Besides, the addition of Si- and Ge-containing aromatic compounds to the above mentioned explosives makes it possible to obtain DNDs with SiV and GeV color centers [69]. However, the prices for TNT and especially for RDX are constantly increasing, which prompted the search for cheaper raw materials.

In [60], (i) pentaerythritol tetranitrate (TEN, 2,2-bis[(nitrooxy)methyl]propane-1,3-diyl dinitrate), (ii) a mixture of Tetryl (2,4,6-trinitrophenylmethyl-nitramine) with 3 wt. % lithium nitrate (LiNO$_3$), (iii) TNT recrystallized from acetone, (iv) picric acid (2,4,6-trinitrophenol) and pure (v) RDX (1,3,5-trinitro-1,3,5-triazinane) were used. Molecular structures of the listed explosives are presented in Fig. 9.

The DND samples under study were obtained by detonating various explosives in a steel blast chamber "Alpha-2M" (Special Design and Technology Bureau "Tekhnolog", St. Petersburg, Russia, working volume 2.14 m^3). Each explosive charge had a mass of 0.5 kg, a diameter of 60 mm, and a length of 108–128 mm (depending on the density of the explosive); it was then packed in a biodegradable polymer bag with water. The explosion took place in an inert environment using distilled water as a coolant, the mass ratio of explosives to water was 1/10.

The details of DND synthesis are summarized in Table 3. DND sample from pentrite (TEN) was synthesized by explosion of pentaerythritol tetranitrate; DND sample from Tetryl with lithium salt – TELi by explosion of a mixture of Tetryl with 3 wt. % lithium nitrate; TNT sample – by explosion of trinitrotoluene recrystallized from acetone; TNP sample – by explosion of picric acid; and RDX sample – by explosion of RDX.
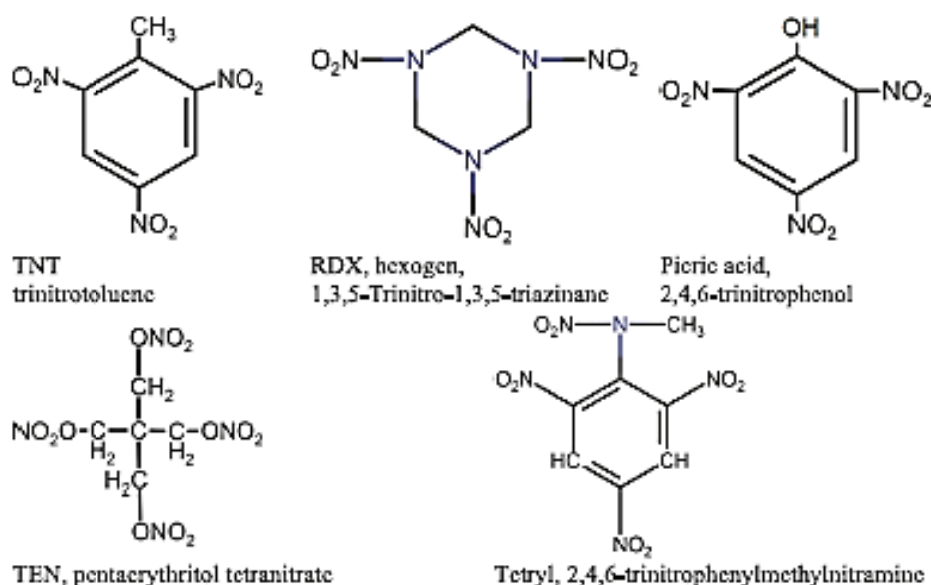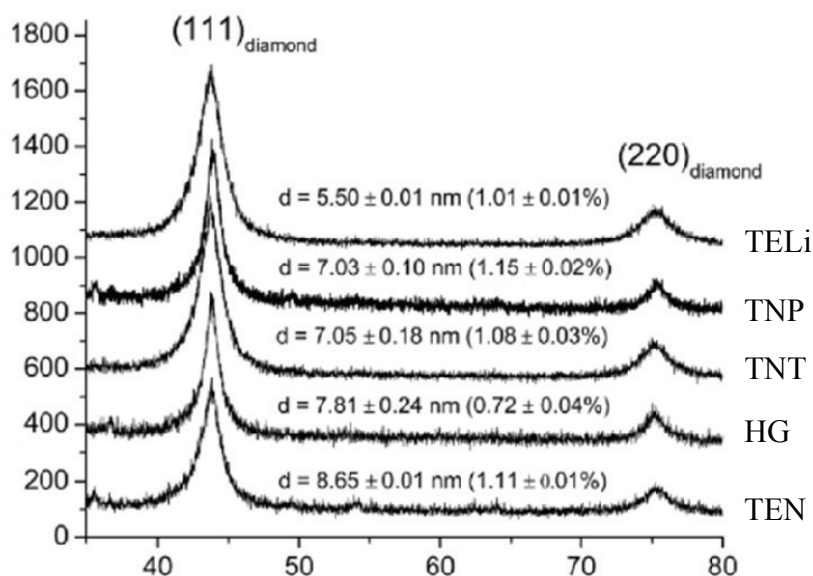

Fig. 9. Molecular structures of explosives [60]

Table 3. Synthesis of the DND samples

Explosive	Charge density, g·cm⁻³	DB yield, wt. %	DND yield, wt. %	DND content in DB, %	Non-combustible impurities, wt. %
TEN	1.59	1.92	0.12	6.25	0.56
TELi	1.63	12.23	4.67	38.19	0.56
TNT	1.58	19.74	0.71	3.66	1.41
TNP	1.57	11.40	1.20	10.53	3.70
RDX	1.61	4.10	0.88	21.46	3.87

Fig. 10. X-ray diffraction spectra of DND samples in the order of crystallite size calculation, with the calculated crystal diameter and the percentage of microstrain indicated in parentheses [70]

The content of total nitrogen in the obtained DNDs ranges from 2.23 to 2.57 wt. %, which is characteristic for most detonation synthesis nanodiamonds [1, 68, 69].

In all X-ray diffraction spectra of the synthesized DNDs (Fig. 10), diffraction maxima were observed at angles $2\theta = 43.7–43.9°$ (avg = 43.8°) (111) and 75.2–75.4° (avg = 75.3°) (220) of reflection of the cubic diamond lattice, respectively (Fig. 10). Small peaks were observed in three of the five samples, apparently due to the presence of residual starting material in the final DND sample. The variation in the observed peak centers reflects the diamond lattices, which are slightly different for each sample and exhibit a range of unit cell parameters, $a_0 = 3.571–3.587$ Å. The observed broadening of the XRD peaks for the DND samples reflects the combined contribution of nanoscale crystallite size and microstress to the width of the XRD peaks [70–74].

The crystallite size range of the DND crystallites from the studied samples was found to be from 5.50 to 8.65 nm with an average value of 7.21 nm and the largest measured dispersion of ±0.24 nm (Fig. 10).

The calculated microstrains range from 0.72 to 1.15 %, which are moderately high values that are also consistent with microstrains measured for other synthetic DND samples using X-ray diffraction analysis [69, 70]. Neither crystallite size nor microstrain directly correlate with DND particle properties measured by EPR or NMR techniques for these samples.

General EPR spectra show intense singlet signals with g ~2.00 as well as broad signals of low intensity with geff < 2.00. The latter vary from sample to sample and are attributed to traces of para- and ferromagnetic impurities. High resolution EPR spectra of intense signals with g ~2.00, typical for DND, have been observed in the investigated DND samples [75, 76].

No correlation of the line widths with the content of magnetic impurities was found. The total content of $S = 1/2$ $N_S = 1/2$ defects varies within the series from 790 to 1832 ppm, gradually increasing in the TEN-TELi-TNT-TNP-RDX series.

Table 4. Experimentally obtained and calculated EPR (columns 2–7)
and ^{13}C NMR (columns 8–10) parameters.

Explosive	$N_{S=1/2}$[a], ppm	ΔH_{pp}^{Nar}[b], mT	ΔH_{pp}^{Br}[c,d], mT	N_{P1}[a,d], ppm	N_{DB}[a,d], ppm	T_{SLe}[e], ms	$\Delta\sigma$[f], kHz	T_{ln}[g], ms	R_{ln}[g], s^{-1}
1	2	3	4	5	6	7	8	9	10
TEN	790	0.55	1.2	258	532	54	2.6	379	2.6
TELi	1372	0.83	1.8	857	515	46	2.5	205	4.9
TNT	1585	0.73	1.6	879	706	26	3.1	110	9.1
TNP	1612	0.68	1.6	1096	516	21	3.8	126	7.9
RDX	1832	1.18	2.4	1265	567	13	5.6	48	20.8

[a] The error in the content of $S = 1/2$ paramagnetic defects $N_S = 1/2$ does not exceed ±15 %.

[b] The error in the narrow EPR line width ΔH_{pp}^{Nar} does not exceed ±0.02 mTl.

[c] Obtained by deconvolution of the experimental EPR spectrum into narrow and broad Lorentzian components.

[d] The error in the width of the broad EPR line ΔH_{pp}^{Br}, does not exceed ±0.1 mTl.

[e] The error in the estimation of the spin-lattice relaxation time of T_{SLe} electrons does not exceed ±35 %.

[f] The error in the estimation of the ^{13}C NMR static line width $\Delta\sigma$ does not exceed ±0.1 kHz.

[g] The error in the ^{13}C nuclear spin-lattice relaxation time of T_{ln} and rate of R_{ln} does not exceed ±10 %.

For the TEN sample, the contribution of defects assigned to P1 centers (N_{P1}) to the total line intensity is significantly lower than for the RDX sample (N_{DB}). The results presented in Table 4 show a gradual increase of N_{P1} in the order TEN-TELi-TNT-TNP-RDX, while NDB remains approximately the same (within the experimental error).

The spin and electron lattice relaxations are approximately the same for all observed paramagnetic particles. Table 4 illustrates the results of such an evaluation performed for each sample examined. The electron relaxation times consistently decrease as the number of paramagnetic defects increases.

In each of the ^1H NMR spectra of the investigated DND samples, two components are detected: (i) a broad component whose width is due to the strong dipole-dipole interaction between the protons of the hydrogen-containing groups of the rigid surface, and (ii) a narrow component attributed to mobile water molecules adsorbed on the DND surface. Such a partially hydrogenated surface is characteristic of most DNDs described in the literature [64]. The separately measured narrow spectral component was obtained with an interpulse delay of 120 μs, which completely attenuates the broad component echo signal. The width of the narrow component increases in the TEN-TELi-TNT-TNP-RDX series, i.e. with increasing number of

paramagnetic nanodiamonds containing paramagnetic defects [64–67].

The intensity of the broad NMR component varied from sample to sample. Its contribution to the total NMR line intensity was maximal for the RDX sample and minimal for TEN. The ratio of the intensities of the narrow and broad NMR components in RDX is 1.8, which means that ~36 % of carbon atoms in the sample belong to disordered shell and surface hydrogen-containing groups, while for TEN this value is ~7%. This fact indicates another noticeable difference in the structure of DND samples obtained from different explosives.

The analysis of the dependency in Fig. 11 (see below) clearly shows that the acceleration of the spin-lattice relaxation of ^{13}C nuclei is associated with an increase in the number of paramagnetic particles in DND particles. On the other hand, the EPR data demonstrate that the content of paramagnetic defects in the surface/boundary layers is almost the same for all samples, while the content of central P1 centers increases. Indeed, in the ^{13}C NMR relaxation measurements, the main contribution to the magnetization comes from the narrow component associated with the carbon nuclei in the core. The nuclei responsible for the defective carbon structure (the broad NMR component) most likely relax at the same rate due to strong interactions between paramagnetic particles in the core and in the shell [75].
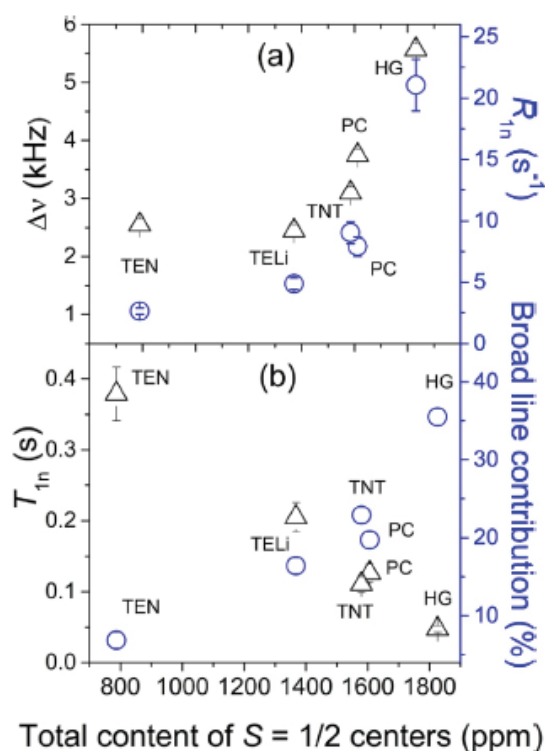
Fig. 11. Dependences of NMR line parameters on the total content of paramagnetic defects $S = 1/2$ in the studied DND samples: *a* – line width Δv – black light triangles, nuclear spin-lattice relaxation rate R_{1n} – light blue circles; *b* – nuclear spin-lattice relaxation time T_{1n} – black unshaded triangles, and relative intensity of the broad Lorentzian component – blue solid circles [75]

All of the distinctive features found in magnetic resonance measurements can be attributed to differences in the structure of DND particles obtained from different explosives and, consequently, to different conditions of their synthesis.

4.2. Molecular structural heterogeneity of DNDs

DNDs are characterized by the presence of a double aggregation system and a stable primary structure [77]. Sedimentation studies determine the size of the latter to be 20–60 nm [78] or 30–50 [55], while light scattering experiments record a size of 100 nm [79, 80].

It is known that DND particles isolated from DB already represent primary structures with a size of 30–50 nm (and in [75] the size is given as 20–60 nm, while light scattering experiments show a size of about 100–200 nm), and fractions with smaller size are absent in such experiments [79, 80].

For all DND samples, characteristic IR sorption was observed for the following functional groups: hydroxyl (O-H) in the wave number regions 3400–3500 cm^{-1}, 1620–1640 cm^{-1}, carbonyl and carboxyl

in the region 1720–1770 cm^{-1}, methyl (–CH$_3$) in the regions 2840–2870 cm^{-1}, 2930–2950 cm^{-1}. The IR sorption features for different DND samples in the 900–1400 cm^{-1} spectral region have been discussed in [79, 80].

The following explosive compositions were used for the detonation synthesis of DND: trinitroresorcin (stifnic acid)/RDX, trinitrobenzene/RDX, trinitrotoluene/RDX, and trinitrophenol (picric acid)/RDX in various mass ratios. Heat treatment experiments of DND samples were performed in weak vacuum (10^{-3} Torr) for 90 min at temperatures of 200, 350, 450, 600, and 900 °C and in air-oxygen atmosphere at temperatures of 100, 350, 700 °C for 60 min. In other words, the authors assume that DNDs consist of structurally inhomogeneous particles of 100–200 nm in size.

The method of high-resolution transmission electron microscopy identifies individual objects up to 4 nm in size, but experiments to determine the particle size by light scattering do not confirm the presence of macroscopic amounts of such fractions.

According to the patent [81], a method for dispersing DND has been developed. DND powder is treated with hydrohalic acid at a temperature of 50–130 °C for 1–10 hours with simultaneous ultrasonic action. The treated powder is washed in deionized water, dried, and annealed in air at 400–450 °C for 1–6 hours. After ultrasonic treatment of the DND suspension, the suspension is centrifuged at an acceleration of at least 12000 g for 0.5–10 hours. The invention makes it possible to obtain a stable monodisperse aqueous suspension of DND particles having a size of 3.9–5.6 nm, free of impurities.

4.3. IR spectrometry

During DND formation, due to the enormous pressure and temperature gradient, diamond crystallites with a defective structure are formed, in which, along with vacancies in the crystal lattice and broken bonds, there are surface inclusions of atoms of chemical elements present in the explosive substance – C, H, N, O. Only nitrogen (~2.5 wt. %) is detected inside the crystal inclusion [82, 83].

Hydrogen, nitrogen and oxygen of the explosive molecules are in the composition of surface functional groups and compounds (CO$_2$, CO, N$_2$, H$_2$O) sorbed by the DND surface. The latter may be located on the accessible surface of the nanodiamond or "bricked up" in the closed pores of the DND particle aggregates. Functional groups are an integral part of the nanodiamond supramolecule, they can be removed or replaced by others, but they are always present on the DND surface.

The efficiency of DND incorporation into composite materials (metal-diamond coatings, polymers, fuels, oils and greases, polishing systems) is directly related to the size of the nanodiamond aggregates and the uniformity of their distribution in the matrix. Mechanical [84], thermochemical [85] and thermal [87] methods are used to destroy the aggregates.

The thermal treatment of DND aggregates is characterized by minimal costs in terms of energy, time and equipment used. The subsequent application of partially disaggregated nanodiamonds is associated with possible chemical reactions of the matrix with functional groups of DND. Therefore, it is very important to determine the composition of functional groups on the surface of modified nanodiamonds.

As a rule, previous works on the IR spectra of nanodiamonds did not trace their history, namely, the peculiarities of the methods of their preparation, chemical purification, the possibility of modification and their influence on the IR spectrum. Manufacturers of DND were rarely mentioned.

The intensity of the intrinsic absorption of the diamond phase in the range of 400–4000 cm^{-1} is low, so the method of IR spectroscopy is quite suitable for the determination of functional groups on the surface of DND.

The IR spectra of the studied diamonds contain absorption bands of hydroxyl groups of both sorbed water molecules (3244–3418 cm^{-1}) and particles bound to the surface (1635–1609 and 3935–3850 cm^{-1}). The absorption bands in the region of 2800–2930 cm^{-1} are due to C–H bond vibrations. Absorption of impurity nitrogen centers in the region of 1558–1566 cm^{-1} was found in natural diamond (1558 cm^{-1}) and dynamically synthesized diamond micropowder (1566 cm^{-1}). Thus, the IR spectroscopy data suggest the presence of different functional groups on the diamond surface.

In [87], IR spectra of DNDs were obtained from a 50/50 mixture of TH (TNT-RDX) and Tetryl (2,4,6-trinitro-N-methyl-N-n-nitroaniline) and subjected to various modifications.

Detonation nanodiamonds obtained by explosion of TNT with RDX (50/50), Tetryl (2,4,6-trinitro-N-methyl-N-n-nitroaniline), their mixtures and, after chemical purification, treated with aqueous ammonia (temperature 220 °C and pressure ~40 atm) [85], air and argon at 430 °C (dry nanodiamond powder) were used as test objects. The DND treatment data are summarized in Table 5.

Despite the fact that all DND samples were subjected to high-temperature treatment: ammonia (albeit in water, sample 1), air, and argon, the IR spectra of the DND samples contain medium-intensity absorption bands in the range of 3300–3390 cm^{-1}, due to valence vibrations of OH– groups, and medium-intensity absorption bands in the range of 1625–1637 cm^{-1}, corresponding to deformation vibrations of OH– groups in water adsorbed on the surface of nanodiamonds. Thus, neither amination in water nor high-temperature treatment of DND surface in active (air) and inert gas medium (argon) likely affects the amount of stubborn OH-groups.

External effects (by ammonia water and gases - air and argon) of dry DND powder and relatively low treatment temperatures (up to 430 °C) failed to make significant changes in the crystal structure of nanodiamonds. Therefore, all samples absorb nitrogen impurity centers intensively at approximately the same frequencies (1103–1124 and 1255–1270 cm^{-1}).

Table 5. The investigated nanodiamonds, producer "Tekhnolog"

No.	DND sample	Treatment
1	Obtained by detonation of TH 50/50 charge in aqueous medium	Treated with NH$_4$OH at temperature 220 °C and pressure 40–50 atm [91] (DND-TAN)
2	Obtained by detonation of TH 50/50 charge in aqueous medium	Heat treatment at 430 °C in air for 2 hours
3	Obtained by detonation of Tetryl charge in aqueous medium	
4	Obtained by detonation of a charge of 70 wt. % Tetryl and 30 wt. % RDX.	Heat treatment at 430 °C in argon for 2 hours
5	Obtained by detonation of a charge of 50 wt. % Tetryl, 30 wt. % TNT and 20 wt. % RDX	

It should be noted that DND-TAN has more nitrogen impurity centers and very strong absorption bands (826, 1328, 1558 cm^{-1}). Exposure of all other DND samples to high temperatures caused a slight decrease in the nitrogen concentration in the DND crystallites due to the possible escape of N_2 beyond the upper 2-3 carbon layers (coordination spheres) of the crystallites. The IR spectrum reflects the state of the surface layer and the upper 2-3 of the coordination spheres.

All other absorption bands: stretching vibrations of adsorbed water (1625–1637 cm^{-1}), > C=O (1742–1790 cm^{-1}), valence vibrations of C_{sp3}–H (2853–2958 cm^{-1}) and valence vibrations of OH– group are present in all five DND samples.

Thus, the effect of temperature (430 °C, 2 h, argon or air) leads to a decrease in the intensity of the absorption bands of nitrogen impurities in DND crystallites due to the possible escape of N_2 beyond the 2-3 upper coordination spheres.

All DND samples obtained from TNT-RDX mixture, Tetryl, mixture of Tetryl with RDX and ternary mixture – TNT, RDX and Tetryl, both treated with aqueous ammonia (220 °C, pressure 40 atm) and gases (argon, air) in the form of dry powders, have the same strong bands of nitrogen impurity centers (826, 1328, 1558 cm^{-1}) (DND-TAN) and ~1110 cm^{-1}, ~1255 cm^{-1} in all samples.

All five samples of the modified DNDs have the same absorption bands of adsorbed water (1625–1637 cm^{-1}), C=O group (1742–1790 cm^{-1}), C_{sp3}–H valence vibrations (2853–2958 cm^{-1}) and OH-group valence vibrations (3330–3397 cm^{-1}) present and pronounced in the IR spectrum.

4.4. Modification of nanodiamonds

In [88], sedimentation and kinetically stable film-forming epoxytitanate sols were synthesized by sol-gel techniques, based on aliphatic epoxy resin EPONEX 1510 and tetrabutoxytitanate solution in acetylacetone and ethyl cellosolve, in the presence of aqueous nitric acid solution and cationic epoxy polymerization catalyst BF_3.

IR spectroscopy shows that weakly hydrolyzable intra-complex titanium compounds are gradually formed in the sols. For more complete opening of epoxy rings and formation of polymeric structure of coatings it is necessary to keep them in air at room temperature for at least 1–2 days. Transparent epoxytitanate coatings obtained by casting or aerography on the surface of optical glass substrates are hydrophilic and have good adhesion to the glass surface (1 point according to the Russian Standard 15140). Modification of epoxytitanate sol with a small amount of detonation nanodiamond (0.2 and 0.4 wt. % of DND) reduces the degree of hydrophilicity of coatings and significantly increases the relative hardness of coatings (from 0.1–0.4 to 0.8–0.9 according to Russian Standard 52166).

Other things being equal, the relative hardness of DND-modified coatings does not depend on the method of coating application, be it airbrush or pouring. However, the relative hardness of coatings without DND applied by airbrush is higher than that of the coatings applied by pouring.

The results of the thermal analysis, combined with the study of the physical and mechanical properties, allow us to conclude that pre-vacuuming and heating the sols up to 80°C, as well as the addition of DND, result in a denser structure of the material coating and increase its thermal resistance. In addition, the introduction of DND into the sols intensifies the hydration processes in the sols. Marine field tests under tropical sea conditions of transparent antifouling epoxy titanate coatings obtained from solutions modified with 0.2 wt. % DND applied to glass surfaces showed that DND can be considered as a mild biocide or synergist that weakly inhibits the process of marine fouling.

5. Conclusion

The optimal range to be observed when designing the process for high yield DND production is shown: pressure in the Chapman-Jouguet plane in the range of 23 to 29 GPa, temperature from 3850 to 4350 K. The composition of the explosives was optimized to obtain DND with a yield of more than 5 wt. %. The small-angle X-ray scattering (SAXS) method allowed to record the appearance and growth of nanocarbon particles just behind the detonation wavefront. A new (fractal) mechanism of DND formation is described, and a predictive method for determining the DND yield from the elemental composition of explosives is shown. It is found that the electrical conductivity in the chemical reaction zone is determined by the carbon content, which forms extended conductive structures.

The main parameters affecting the yield of DND are described, the optimum being the use of armor (shell) from an aqueous solution of urotropine or urea or hydrazine. Results on the DND yield using picric acid, Tetryl and its binary and ternary charges are given, and it is shown that Tetryl and its mixtures are fully competitive with respect to the currently used mixtures of TNT with RDX. Comprehensive EPR and NMR properties of DND obtained by detonation

of pentaerythritol tetranitrate, Tetryl with lithium nitrate, high purity TNT, picric acid and pure RDX are given. Regardless of the type of surface modification of DND particles, the same sorption bands of adsorbed water (1625–1637 cm^{-1}), C=O group (1742–1790 cm^{-1}), C$_{sp3}$–H valence vibrations (2853–2958 cm^{-1}) and OH group valence vibrations (3330–3397 cm^{-1}) are present and prominent in the IR spectrum. Antifouling epoxy-titanium coatings prepared from the solutions modified with 0.2 wt. % DND showed that DND could be considered as a mild biocide or synergist that weakly inhibited the marine fouling process of surfaces.

6. Funding

7. Conflict of interest

The authors declare no conflicts of interest.

References

1. Dolmatov VY. *Detonation nanodiamonds. Preparation, properties, application*. Saint-Petersburg: Professional; 2011. 534 p. ISBN: 978-5-91259-073-3. (In Russ.)

2. Vul' A, Shenderova O Eds. *Detonation Nanodiamonds: Science and Applications*. New York: Jenny Stanford Publishing; 2014. 346 p. ISBN: 978-0-429-16896-3.

3. Shenderova OA, Gruen DM. *Ultrananocrystalline Diamond: Synthesis, Properties, and Applications*. William Andrew; 2006. 621 p. ISBN: 978-0-8155-1942-3.

4. Lisichkin GV, Olenin AYu, Kulakova II. *Surface modification of inorganic nanoparticles*. Moscow: Technosphere; 2020. 394 p.

5. Van Thiel M, Ree FH. Properties of carbon clusters in TNT detonation products: graphite-diamond transition. *Journal ofApplied Physics*. 1987;62(5):1761-1767. DOI:10.1063/1.339575

6. Dremin AN, Pershin SV, Pyatiernev SV, Tsaplin DN. On the fracture of the dependence of the detonation velocity on the initial density of TNT. *Fizika goreniya i vzryva = Combustion, Explosion, and Shock Waves.* 1989;25(5):141-144. (In Russ.)

7. Antipenko A G, Pershin SV, Tsaplin DN. Dynamic studies of diamond formation in TNT detonation products. *Proceedings 10th International Conference on High Energy Rate Fabrication. Ljubljana,* Yugoslavia; 1989. p. 170-178. (In Russ.)

8. Pershin SV, Tsaplin DN, Antipenko AG. On the possibility of diamond formation during tetrile detonation. *5th All-Union Conference on Detonation. Krasnoyarsk,* Chernogolovka: OIHF; 1991. p. 233-236, V.2. (In Russ.)

9. Pershin ST, Tsaplin DN. Dynamic studies of detonation synthesis of dense phases of matter. *5th All-Union Conference on Detonation. Krasnoyarsk,* Chernogolovka: OIHF; 1991. p. 237-244, V.2. (In Russ.)

10. Dolmatov VYu, Dorokhov AO, Mullumaki V, Vehanen A, Marchukov VA. Zone of chemical reactions at detonation synthesis of nanodiamonds on the phase diagram of carbon. *Proceedings of XXII International Conference 'Rock-destroying and metal-working tools – technique and technology of their manufacture and application'*. Kiev: V.N. Bakul ISM; 2019. B. 22. p. 199-204. (In Russ.)

11. Dolmatov VYu, Rudenko DV, Lisitsin ON, Kiselev MN, et al. *A method of obtaining detonation nanodiamonds*. Russian Federation patent 2,712,551. 29 January 2020. (In Russ.)

12. Zhukov BP. *Energetic condensed systems*. Moscow: Janus-K; 2000. 299 p. (In Russ.)

13. Dolmatov VYu. Assessment of the applicability of explosive charges for the synthesis of detonation nanodiamonds. *Sverkhtverdyye materialy = Journal of Superhard Materials.* 2016;5:109-113. (In Russ.)

14. Dolmatov V. Specific power of explosive and its effect on nanodiamonds. *Universal Journal of Carbon Research*. 2023;66-71. DOI:10.37256/ujcr.1220233919

15. Blinova MA, Dolmatov VYu. Prognostic estimation of detonation nanodiamonds yield from oxygen balance of high-power carbon-containing explosives. *Third International Symposium Chemistry for Biology, Medicine, Ecology and Agriculture: Collection of Abstracts, St. Petersburg, 5-7 June 2024*. St. Petersburg: LEMA Publ. House; 2024. p. 100-102. (In Russ.)

16. Aleshayev AN, Zubkov PI, Kulipanov GN, Lukyanchikov LA, et al. Application of synchrotron radiation to study detonation and shock-wave processes. *Fizika goreniya i vzryva = Combustion, Explosion, and Shock Waves.* 2001;37(5):104-113. (In Russ.)

17. Titov VM, Tolochko BP, Ten KA, Lukyanchikov LA, et al. Where and when are nanodiamonds formed under explosion? *Diamond and Related Materials*. 2007;16(12):2009-2013. DOI:10.1016/j.diamond.2007.09.001

18. Dolmatov VYu, Myllymäki V, Vehanen A. A possible mechanism of nanodiamond formation during detonation synthesis. *Journal of Superhard Materials*. 2013;35(3):143-150. DOI:10.3103/S1063457613030039

19. Dolmatov VY, Rudometkin KA. Probable mechanism of detonation nanodiamond formation. *Izvestiya Sankt-Peterburgskogo gosudarstvennogo tekhnologicheskogo instituta (tekhnicheskogo universiteta)*. 2013;(21(47)):106-109. (In Russ.)

20. Sattler KD. *Carbon nanomaterials sourcebook*. New York: CRC Press, Taylor & Francis Group; 2016. 614 p. ISBN: 978-1-4822-5268-2.

21. Dolmatov VYu, Ozerin AN, Eidelman ED, Dorokhov AO. Predictive evaluation of the effect of the yield of detonation nanodiamonds depending on their elemental composition. *Extreme states of substance. Detonation. Shock waves. International Conference XXIII Khariton's Topical Scientific Readings. Abstracts.* Sarov: RFNC-VNIIEF; 2022. p. 36-37 (In Russ.)

22. Ershov AP, Andreev VV, Kashkarov AO, Luk'yanov YL, et al. Detonation of ultrafine explosives. *Combustion, Explosion, and Shock Waves.* 2021;57(3):356-363. DOI:10.1134/S0010508221030114

23. Ershov AP, Satonkina NP, Plastinin AV, Yunoshev AS. Diagnostics of the chemical reaction zone in detonation of solid explosives. *Combustion, Explosion, and Shock Waves.* 2020;56(6):705-715. DOI:10.1134/S0010508220060106

24. Satonkina NP, Medvedev DA. On the kinetics of chemical reactions at the detonation of organic high explosives. *Physics of Fluids.* 2022;34(8):087113. DOI:10.1063/5.0095053

25. Koenig M, Benuzzi-Mounaix A, Ravasio A, Vinci T, et al. Progress in the study of warm dense matter. *Plasma Physics and Controlled Fusion.* 2005;47(12B):B441-B449. DOI:10.1088/0741-3335/47/12B/S31

26. Satonkina NP. The dynamics of carbon nanostructures at detonation of condensed high explosives. *Journal of Applied Physics.* 2015;118(24):245901. DOI:10.1063/1.4938192

27. Satonkina NP. Correlation of electrical conductivity in the detonation of condensed explosives with their carbon content. *Combustion, Explosion, and Shock Waves.* 2016;52(4):488-492. DOI:10.1134/S0010508216040134

28. Satonkina NP. Chemical composition of detonation products of condensed explosives and its relationship to electrical conductivity. *Journal of Physics: Conference Series.* 2018;946:012059. DOI:10.1088/1742-6596/946/1/012059

29. Ershov AP, Satonkina NP, Dibirov OA, Tsykin SV, et al. A study of the interaction between the components of heterogeneous explosives by the electrical-conductivity method. *Combustion, Explosion, and Shock Waves.* 2000;36(5):639-649. DOI:10.1007/BF02699528

30. Satonkina NP, Ershov AP, Kashkarov AO, Rubtsov IA. Elongated conductive structures in detonation soot of high explosives. *RSC Advances.* 2020;10(30):17620-17626. DOI:10.1039/D0RA01393E

31. Dolmatov VYu, Ozerin AN, Kulakova II, Bochechka OO, et al. Detonation nanodiamonds: new aspects in the theory and practice of synthesis, properties and applications. *Russian Chemical Reviews.* 2020;89(12):1428-1462. DOI:10.1070/RCR4924

32. Dolmatov VY. *Diamond-carbon material and method of its obtaining.* Russian Federation patent 2,359,902. 27 June 2008. (In Russ.)

33. Dolmatov VYu, Vehanen A, Myllymäki V, Kozlov AS, et al. Effect of armoring composition on the yield of nanodiamonds and content of impurities. *Russian Journal of Applied Chemistry.* 2018;91(2):225-229. DOI:10.1134/S107042721802009X

34. Dorokhov AO, Dolmatov VYu, Malygin AA, Kozlov AS, et al. Development of the detonation nanodiamond synthesis from tetryl based ternary mixtures. *Russian Journal of Applied Chemistry.* 2020;93(7):1083-1089. DOI:10.1134/S1070427220070204

35. Dolmatov VY, Rudenko DV Lisitsin ON, Kiselev MN, et al. *Method of obtaining detonation nanodiamonds.* Russian Federation patent 2,703,212. 15 October 2019. (In Russ.)

36. Dolmatov VY, Rudenko DV Lisitsin ON, Kiselev MN, et al. *Method of obtaining detonation nanodiamonds.* Russian Federation patent 2,711,599. 17 October 2019. (In Russ.)

37. Dolmatov VYu, Malygin AA, Dorokhov AO, Kozlov AS, et al. Development of a process for producing detonation nanodiamonds from tetryl and binary compositions based on it. *Journal of Superhard Materials.* 2020;42(3):145-156. DOI:10.3103/S1063457620030053

38. Dolmatov VY, Rudenko DV,Lisitsin ON, Kiselev MN, Dorokhov AO, Denisov IV. *Method of obtaining detonation nanodiamonds.* Russian Federation patent 2,712,551. 29January 2020. (In Russ.)

39. Antipenko, AG, Yakushev, VV. Nature of electrical conductivity of detonation products of condensed explosives. *Detonation. Proceedings of the 5th All-Union Symposium on Combustion and Explosion. Dremin A.N. Odessa, 1977.* Chernogolovka: OIChF, USSR Academy of Sciences.; 1977. p. 93-96.

40. Marchukov VA, Kolodyazhny AL, Makarov IA, Korolev KM, Sushchev VG. *Method of purification of detonation nanodispersed diamonds.* Russian Federation patent 2,599,665. 10 October 2016. (In Russ.)

41. Shilova OA, Kopitsa GP, Khamova TV, Gorshkova SE, et al. Morphology and structure of boron-doped detonation nanodiamond charge. *Fizika i khimiya stekla = Glass Physics and Chemistry.* 2022;48(1):52-62. DOI:10.31857/S0132665122010140 (In Russ.)

42. Vul AYa, Shenderova OA. *Detonation nanodiamonds. Technology, structure, properties and applications.* St. Petersburg: A.F. Ioffe FTI; 2016. 381 p.

43. Volkov DS, Proskurnin MA, Korobov MV. Elemental analysis of nanodiamonds by inductively-coupled plasma atomic emission spectroscopy. *Carbon.* 2014;74:1-13. DOI:10.1016/j.carbon.2014.02.072

44. Korobov MV, Volkov DS, Avramenko NV, Belyaeva LA, et al. Improving the dispersity of detonation nanodiamond: differential scanning calorimetry as a new method of controlling the aggregation state of nanodiamond powders. *Nanoscale.* 2013;5(4):1529. DOI:10.1039/c2nr33512c

45. Volkov DS, Proskurnin MA, Korobov MV. Survey study of mercury determination in detonation nanodiamonds by pyrolysis flameless atomic absorption spectroscopy. *Diamond and Related Materials.* 2014;50:60-65. DOI:10.1016/j.diamond.2014.08.013

46. Dolmatov VYu, Shames AI, Ōsawa E, Vehanen A, et al. Detonation nanodiamonds: from synthesis theory to application practice. *Journal of Advanced Materials and Technologies.* 2021;6(1):54-80. DOI:10.17277/jamt.2021.01.pp.054-080

47. Kulakova II, Korol'kov VV, Yakovlev RYu, Lisichkin GV. The structure of chemically modified detonation-synthesized nanodiamond particles. *Nanotechnologies in Russia.* 2010;5(7-8):474-485. DOI:10.1134/S1995078010070074

48. Vereshchagin AL, Yur'ev GS. Structure of detonation diamond nanoparticles. *Inorganic Materials*. 2003;39(3):247-253. DOI:10.1023/A:1022621407325

49. Dolmatov VYu. Some speculations as to the structure of a cluster of a detonation-produced nanodiamond. *Sverkhtverdyye materialy = Journal of Superhard Materials*. 2005;(1):28-32. (In Russ.)

50. Kulakova II. Surface modification and physicochemical properties of nanodiamonds [8 mm] Surface chemistry of nanodiamonds. *Fizika tverdogo tela = Physics of the Solid State*. 2004;46(4):621-628. (In Russ.)

51. Yakovlev RYu, Dogadkin NN, Kulakova II, Lisichkin GV, et al. Determination of impurities in detonation nanodiamonds by gamma activation analysis method. *Diamond and Related Materials*. 2015;55:77-86. DOI:10.1016/j.diamond.2015.03.010

52. Kulakova II, Korolkov BB, Yakovlev RY, Lisichkin GV. Structure of particles of chemically modified nanodiamond of detonation synthesis. *Rossiyskiye Nanotekhnologii = Nanobiotechnology Reports*. 2010;5(7-8):66-73. (In Russ.)

53. Tsubota T, Urabe K, Egawa S, Takagi H, et al. Surface modification of hydrogenated diamond powder by radical reactions in chloroform solutions. *Diamond and Related Materials*. 2000;9(2):219-223. DOI:10.1016/S0925-9635(00)00234-X

54. Dolmatov VYu, Yur'ev GS, Myllymäki V, Korolev KM. Why detonation nanodiamonds are small. *Journal of Superhard Materials*. 2013;35(2):77-82. DOI:10.3103/S1063457613020020

55. Ando T, Rawles RE, Yamamoto K, Kamo M, et al. Chemical modification of diamond surfaces using a chlorinated surface as an intermediate state. *Diamond and Related Materials*. 1996;5(10):1136-1142.

56. Liang Y, Ozawa M, Krueger A. A general procedure to functionalize agglomerating nanoparticles demonstrated on nanodiamond. *ACS Nano*. 2009;3(8):2288-2296. DOI:10.1021/nn900339s

57. Zheng W-W, Hsieh Y-H, Chiu Y-C, Cai S-J, et al. Organic functionalization of ultradispersed nanodiamond: synthesis and applications. *Journal of Materials Chemistry*. 2009;19(44):8432. DOI:10.1039/b904302k

58. Christiaens P, Vermeeren V, Wenmackers S, Daenen M, et al. EDC-mediated DNA attachment to nanocrystalline CVD diamond films. *Biosensors and Bioelectronics*. 2006;22(2):170-177. DOI:10.1016/j.bios.2005.12.013

59. Koshcheev AP. Modesorption mass spectrometry in the light of solving the problem of passportisation and unification of surface properties of detonation nanodiamonds. *Rossiyskiy Khimicheskiy Zhurnal = Russian Journal of General Chemistry*. 2008;52(5):88-96. (In Russ.)

60. Shames AI, Panich AM, Friedlander L, Dolmatov VYu. Magnetic resonance study of novel detonation nanodiamonds originated from non-conventional explosives. *Diamond and Related Materials*. 2023;136:110059. DOI:10.1016/j.diamond.2023.110059

61. Shenderova OA, McGuire GE. Science and engineering of nanodiamond particle surfaces for biological applications (review). *Biointerphases*. 2015;10(3):030802. DOI:10.1116/1.4927679

62. Arnault JC. Surface modifications of nanodiamonds and current issues for their biomedical applications. *Novel Aspects of Diamond*. Cham: Springer International Publishing; 2015. p. 85-122.

63. Komatsu N. Chemical functionalization of nanodiamond for nanobiomedicine. *Synthesis and Applications of Nanocarbons*. Wiley; 2020. p. 229-246.

64. Panich AM. Nuclear magnetic resonance studies of nanodiamond surface modification. *Diamond and Related Materials*. 2017;79:21-31. DOI:10.1016/j.diamond.2017.08.013

65. Dubois M, Guérin K, Petit E, Batisse N, et al. Solid-state NMR study of nanodiamonds produced by the detonation technique. *The Journal of Physical Chemistry C*. 2009;113(24):10371-10378. DOI:10.1021/jp901274f

66. Donnet J-B, Fousson E, Delmotte L, Samirant M, et al. 13C NMR characterization of nanodiamonds. *ComptesRendus de l'Académie des Sciences – Series IIC – Chemistry*. 2000;3(11-12):831-838. DOI:10.1016/S1387-1609(00)01208-1

67. Alam TM. Solid-state magic angle spinning NMR spectroscopy characterization of particle size structural variations in synthetic nanodiamonds. *Materials Chemistry and Physics*. 2004;85(2-3):310-315. DOI:10.1016/j.matchemphys.2004.01.029

68. Dolmatov VY, Sushchev VG, Marchukov VA. *Method of isolation of synthetic ultradisperse diamonds*. Russian Federation patent 2,109,683. 05 March 1996.

69. Dolmatov VY. Detonation-synthesis nanodiamonds: synthesis, structure, properties and applications. *Russian Chemical Reviews*. 2007;76(4):339-360. DOI:10.1070/RC2007v076n04ABEH003643

70. Makino Y, Yoshikawa T, Tsurui A, Liu M, et al. Direct synthesis of group IV-vacancy center-containing nanodiamonds via detonation process using aromatic compound as group IV element source. *Diamond and Related Materials*. 2022;130:109493. DOI:10.1016/j.diamond.2022.109493

71. Stehlik S, Henych J, Stenclova P, Kral R, et al. Size and nitrogen inhomogeneity in detonation and laser synthesized primary nanodiamond particles revealed via salt-assisted deaggregation. *Carbon*. 2021;171:230-239. DOI:10.1016/j.carbon.2020.09.026

72. Chen P, Huang F, Yun S. Characterization of the condensed carbon in detonation soot. *Carbon*. 2003;41(11):2093-2099. DOI:10.1016/S0008-6223(03)00229-X

73. Chen P, Huang F, Yun S. Structural analysis of dynamically synthesized diamonds. *Materials Research Bulletin*. 2004;39(11):1589-1597. DOI:10.1016/j.materresbull.2004.05.009

74. Stehlik S, Mermoux M, Schummer B, Vanek O, et al. Size effects on surface chemistry and Raman spectra of sub-5 nm oxidized high-pressure high-temperature and detonation nanodiamonds. *The Journal of Physical Chemistry C*. 2021;125(10):5647-5669. DOI:10.1021/acs.jpcc.0c09190

75. Shames AI, Panich AM. *Nanodiamonds: Advanced Material Analysis, Properties and Applications*. William Andrew; 2017. 506 p. ISBN: 978-0-323-43032-6.

76. Shames AI, Zegrya GG, Samosvat DM, Osipov VY, Vul' AYa. Size effect in electron paramagnetic resonance spectra of impurity centers in diamond particles. *Physica E: Low-dimensional Systems and Nanostructures*. 2023;146:115523. DOI:10.1016/j.physe.2022.115523

77. Korets AYa Krylov AS, Mironov EV. Molecular structural heterogeneity of ultradisperse diamond-containing material and the reasons for its occurrence. *Khimicheskaya Fizika = Russian Journal of Physical Chemistry B*. 2007;26(7):58-66. (In Russ.)

78. Sakovich GV, Gubarevich VD, Badaev FZ, Brylyakov PM, et al. Aggregation of diamonds obtained from explosives. *Doklady Akademii nauk = Doklady Biochemistry*. 1990;310(2):402-404. (In Russ.)

79. Mironov E. Chemical aspect of ultradispersed diamond formation. *Diamond and Related Materials*. 2003;12(9):1472-1476. DOI:10.1016/S0925-9635(03)00177-8

80. Korets AYa, Krylov AS, Mironov EV. Molecular structural nonuniformity of ultradispersed diamond-containing material and the reasons why it arises. *Russian Journal of Physical Chemistry B*. 2007;2(5):485-492. DOI:10.1134/S1990793107050077

81. Alekensky AE, Vul AY, Dideykin AT. *Method of obtaining aqueous suspension of detonation nanodiamonds*. Russian Federation patent 2,446,097. 27 March 2012.

82. Kulakova II. Surface chemistry of nanodiamonds. *Physics of the Solid State*. 2004;46(4):636-643. DOI:10.1134/1.1711440

83. Kulakova II, Korolkov VV, Yakovlev RY, Karpukhin AV, Lisichkin GV Structure of particles of chemically modified nanodiamond of detonation synthesis. *XII International Conference 'Rock-destroying and metal-forming tools – technique and technology of their manufacture and application'. Morskoye settlement, Crimea. September 2009*. Kiev: V.N. Bakul ISM; 2009. V. 12. p. 299-305. (In Russ.)

84. Popov VA, Kobelev AG, Chernyshev VN. *Nanopowders in composite production*. Moscow: Intermet Engineering; 2007. 336 p. (In Russ.)

85. Dolmatov VYu, Marchukov VA, Sushchev VG, Veretennikova MV. *Method of obtaining a stable suspension of detonation nanodiamonds*. Russian Federation patent 2,384,524. 10 November 2009.

86. Vul' AYa. *Detonation nanodiamonds. Technology, structure, properties and applications*. St. Petersburg: A.F. Ioffe Institute of Physics and Technology; 2016. 381 p. ISBN: 978-5-93634-025-3.

87. Dolmatov VY, Ozerin AN, Voznyakovsky AP, Voznyakovsky AA, et al. Infrared spectrometry of modified detonation nanodiamonds. *Izvestiya Sankt-Peterburgskogo gosudarstvennogo tekhnologicheskogo instituta (tekhnicheskogo universiteta)*. 2023;66 (92):31-34. DOI:10.36807/1998-9849-2023-66-92-31-34

88. Shilova OA, Glebova IB, Voshchikov VI, Ugolkov VL, et al. Environmentally friendly antifouling transparent coatings based on sol-gel "epoxy/titanium tetrabutoxide" composition modified with detonation nanodiamond. *Journal of Advanced Materials and Technologies*. 2022;7(3):201-218. DOI:10.17277/jamt.2022.03.pp.201-218

Information about the authors / Информация об авторах

Valerii Yu. Dolmatov, D. Sc. (Eng.), Head of research laboratory, Special Construction and Technology Bureau "Technolog", St. Petersburg, Russian Federation; ORCID 0000-0001-8643-0404; e-mail: diamondcentre@mail.ru

Dmitry V. Rudenko, Cand. Sc. (Econ.), Director-Chief Designer, Special Construction and Technology Bureau "Technolog", St. Petersburg, Russian Federation; e-mail: rudenko@sktb-technolog.ru

Maxim N. Kiselev, General Director, JSC "Plant "Selmash", Kirov, Russian Federation; e-mail: maksimel1977-77@mail.ru

Nataliya P. Satonkina, D. Sc. (Phys. and Math.), Senior Researcher, Lavrentiev Institute of Hydrodynamics, Siberian Branch of RAS, Novosibirsk; Russian Federation; ORCID 0000-0002-5894-7497; e-mail: n.satonkina@g.nsu.ru

Долматов Валерий Юрьевич, доктор технических наук, начальник научно-исследовательской лаборатории, Специальное конструкторско-технологическое бюро «Технолог», Санкт-Петербург, Российская Федерация; ORCID 0000-0001-8643-0404; e-mail: diamondcentre@mail.ru

Руденко Дмитрий Владимирович, кандидат экономических наук, директор, главный конструктор, Специальное конструкторско-технологическое бюро «Технолог», Санкт-Петербург, Российская Федерация; e-mail: rudenko@sktb-technolog.ru

Киселев Максим Николаевич, генеральный директор, АО «Завод «Сельмаш», Киров, Российская Федерация; e-mail: maksimel1977-77@mail.ru

Сатонкина Наталья Петровна, доктор физико-математических наук, старший научный сотрудник, Институт гидродинамики им. М. А. Лаврентьева СО РАН, Новосибирск, Российская Федерация; ORCID 0000-0002-5894-7497; e-mail: n.satonkina@g.nsu.ru

Natalia M. Lapchuk, Cand. Sc. (Phys. and Math.), Associate Professor, Belarusian State University, Minsk, Belarus; Scopus ID 6506141523; e-mail: lapchuk@bsu.by

Maria A. Blinova, third category research engineer, Special Construction and Technology Bureau "Technolog", Student, State Institute of Technology Saint-Petersburg Russia, St. Petersburg, Russian Federation; ORCID 0009-0004-4224-0755; e-mail: mashablinova5@gmail.com

Vladimir T. Senyut, Cand. Sc. (Eng.), Leading Researcher, The Joint Institute of Mechanical Engineering of the NAS of Belarus, Minsk, Belarus; ORCID 0000-0002-1595-8516; e-mail: vsenyut@tut.by

Sergey D. Pisarevsky, Cand. Sc. (Military), Chief Researcher, Geoinformation Systems of the NAS of Belarus, Minsk, Belarus; e-mail: pi_sar@mail.ru

Alla V. Nozhkina, D. Sc. (Chem.), Scientific Supervisor, JSC "Research Institute of Natural, Synthetic Diamonds and Tools", Moscow, Russian Federation; ORCID 0000-0003-4750-2625; e-mail: nojkina@inbox.ru

Alexander P. Ershov, Cand. Sc. (Phys. and Math.), Senior Researcher, Lavrentiev Institute of Hydrodynamics, Siberian Branch of RAS, Novosibirsk, Russian Federation; ORCID 0000-0003-2306-1837; e-mail: ershov.d.s@yandex.ru

Лапчук Наталья Михайловна, кандидат физико-математических наук, доцент, Белорусский государственный университет, Минск, Республика Беларусь; Scopus ID 6506141523; e-mail: lapchuk@bsu.by

Блинова Мария Алексеевна, инженер-исследователь третьей категории, Специальное конструкторско-технологическое бюро «Технолог», студент, Санкт-Петербургский государственный технологический институт (технический университет), Санкт-Петербург, Российская Федерация; ORCID 0009-0004-4224-0755; e-mail: mashablinova5@gmail.com

Сенють Владимир Тадеушевич, кандидат технических наук, ведущий научный сотрудник, Объединенный институт машиностроения НАН Беларуси, Минск, Республика Беларусь; ORCID 0000-0002-1595-8516; e-mail: vsenyut@tut.by

Писаревский Сергей Дмитриевич, кандидат военных наук, главный научный сотрудник, УП «Геоинформационные системы» НАН Беларуси, Минск, Республика Беларусь; e-mail: pi_sar@mail.ru

Ножкина Алла Викторовна, доктор химических наук, научный руководитель, ОАО «Научно-исследовательский институт природных, синтетических алмазов и инструмента», Москва, Российская Федерация; ORCID 0000-0003-4750-2625; e-mail: nojkina@inbox.ru

Ершов Александр Петрович, кандидат физико-математических наук, старший научный сотрудник, Институт гидродинамики имени М. А. Лаврентьева СО РАН, Новосибирск, Российская Федерация; ORCID 0000-0003-2306-1837; e-mail: ershov.d.s@yandex.ru